**Aus dem Zentrum für Neurologie Tübingen**
**Neurologische Klinik und Hertie-Institut für klinische Hirnforschung**
**Abteilung für Zellbiologie Neurologischer Erkrankungen am HIH**
**(Hertie-Institut)**
**Leiter: Professor Dr. M. Jucker**

# Modulation of Alzheimer's Pathology in Transgenic Mouse Models

**Inaugural-Dissertation**
**zur Erlangung des Doktorgrades**
**der Medizin**

**der Medizinischen Fakultät**
**der Eberhard Karls Universität**
**zu Tübingen**

**vorgelegt von**

**Carmen Cecilia Duma**

**aus**

**Oradea, Rumänien**

**2009**

| | |
|---|---|
| Dekan: | Professor Dr. I. B. Autenrieth |
| 1. Berichterstatter | Professor Dr. M. Jucker |
| 2. Berichterstatter | Professor Dr. G. Buchkremer |

# Abbreviations

| | |
|---|---|
| Aβ | beta-amyloid |
| ACE | angiotensin converting enzyme |
| AD | Alzheimer's disease |
| Aph-1 | anterior pharynx defective-1 |
| ApoE | apolipoprotein E |
| APP | amyloid precursor protein |
| BACE | β-site of APP cleaving enzyme |
| CAA | cerebral amyloid angiopathy |
| Cdk5 | cyclin-dependent kinase 5 |
| DNA | deoxyribonucleic acid |
| FAD | familial Alzheimer's disease |
| FTDP-17 | frontotemporal dementia and parkinsonism linked to chromosome 17 |
| GSK3β | glycogen synthase kinase β |
| IDE | insulin degrading enzyme |
| LRP | low density lipoprotein receptor-related protein |
| MARK | microtubule-affinity-regulating kinase |
| MT(s) | microtubule(s) |
| NFT(s) | neurofibrillary tangle(s) |
| NSAIDs | non-steroidal anti-inflammatory drugs |
| Pen-2 | presenilin enhancer-2 |
| PS1 | presenilin-1 |
| PS2 | presenilin-2 |

# Table of contents

# 1. Introduction

## 1.1 Epidemiological aspects of dementia

Dementia is the clinical syndrome characterized by acquired and persistent decline in cognitive function, in an alert individual. It is of sufficient severity to interfere with daily functioning and the quality of life. The memory capacity and one other area of cognition such as verbal functions, visuospatial abilities, emotional outbursts, attention or executive functions are affected *(1).*

In dementia, neither the pathology nor the cognitive deficits are truly global or diffuse. Every disorder causing dementia has an affinity for certain parts of the nervous system, and most dementia forms have relative neuropsychological focality, at least in their early stages *(2).*

There are several different forms that dementia can take on. The most common type is Alzheimer's disease that accounts for 50-75% of cases of dementia, followed by vascular dementia. Approximately 7% of people worldwide older than 65, and to 40% in their 80's suffer from Alzheimer's disease *(3).* Other disorders, less common, that cause dementia include: Dementia with Lewy bodies, Fontotemporal dementia, Alcohol dementias (Korsakoffs syndrome), and HIV/AIDS-related dementia.

There is a slightly higher prevalence rate of Alzheimer's disease in women and a trend towards more vascular dementia in men. The vascular dementia is more common compared with AD in Japanese and Russian studies *(4-7).*

Because of ageing of the world's population, in the future there will be an increase in the numbers of people with dementia, as a simple consequence of an increase in the size of the population most at risk *(8).*

There are currently an estimated 24 million people with dementia in the world, with 4,6 million new cases of dementia every year (one new case every 7 seconds). This amount will double every 20 years, to 42 million by 2020 and 81 million by 2040. Most people with dementia live in developing countries: 60% in 2001 and this number is projected to increase to 71% by 2040 *(9).*

The impact of dementia on individuals, families and health-care systems is

considerable, and in the absence of effective prevention or treatment this will continue to increase *(10).*

## 1.2 Alzheimer's disease

### 1.2.1 Genetics

As a chronic condition, Alzeimer's disease seems to have at the origin a long-term complex multifactorial process. Susceptibility to Alzheimer's disease (AD) is governed by multiple genetic and environmental factors that interact all through life *(11).*

The age of onset allows demarcation of Alzheimer's disease as early or familial AD (FAD) below the age of 65 years, and late or sporadic after 65 years onset.

Less than 5% suffer from FAD, while sporadic form of the disease is responsible for the largest proportion of cases *(12).* Autosomal dominant mutations in at least three different genes, that encode the amyloid precursor protein (APP) or the presenilins 1, 2 (PS1 and PS2) can cause early onset AD *(13).* APP mutations account for 2%-3% and *PS-1* mutations for about 50% to 80% of FAD while *PS-2* mutations are very rare (Fig. 1).

The first genetic mutation connected with early-onset AD was in the APP gene, located on the long (q) arm of chromosome 21 at position 21. Suspicions that Chromosome 21 may be implicated in the etiology of Alzheimer's disease appeared by the discovery that some families in which Alzheimer's disease is inherited as an autosomal dominant mutation produce a significantly higher than normal number of Down syndrome (Trisomy 21) *(14).* This lead to the first genetic linkage discovery between a locus on chromosome 21q and early-onset familial AD. The screening of the sequenced APP gene showed the presence of several missense mutations *(15, 16).*

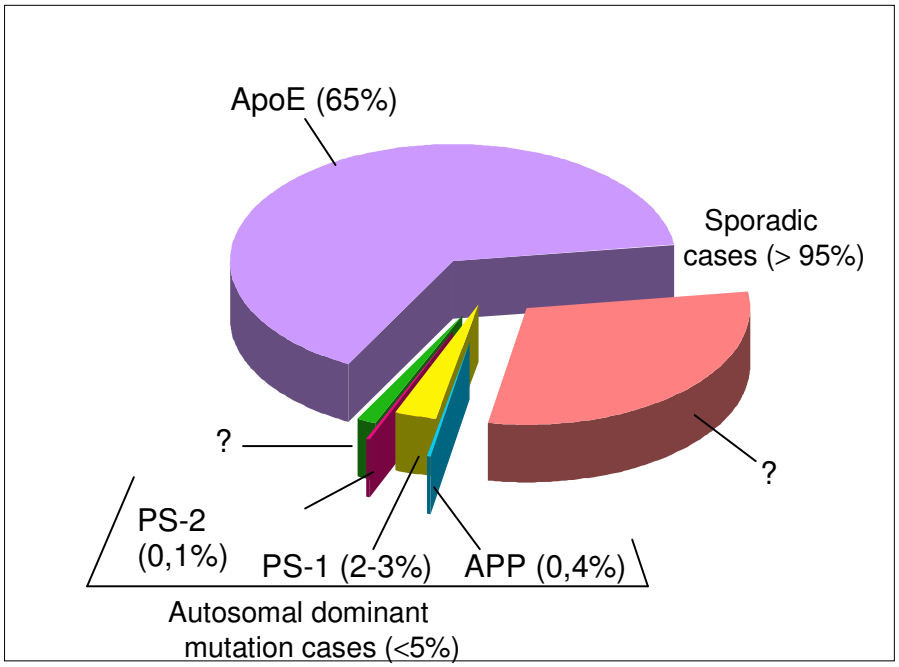


**Fig. 1.** Distribution of Alzheimer's disease forms and their related genetic susceptibility factors *(adapted from (11)).*

Mutations have been identified also in presenilin 1 (PS1) on chromosome 14 *(17)* and presenilin 2 (PS2) on chromosome 1 *(18).* There are more than 120 different missense mutations discovered in the PS1 gene (http://molgen-www.uia.ac.be/ADMutations/), and only 8 in PS2.

Lately, several genetic susceptibility factors that increase the risk of developing sporadic AD have been discovered. These include the ε4 allele of the apolipoprotein E (apoE) on chromosome 19, the proteinase inhibitor α2-macroglobulin gene on chromosome 12, low density lipoprotein receptor-related protein (LRP), angiotensin converting enzyme (ACE) or insulin degrading enzyme (IDE) gene on chromosome 10.

No mutation in the tau gene has been yet identified in Alzheimer's disease, but in FTDP-17 (Frontotemporal dementia and parkinsonism linked to chromosome 17), an autosomal dominant neurodegenerative disorder characterized by the accumulation of neurofibrillary tangles in affected brain regions, more than 20 different mutations in the human tau on chromosome 17 have been described. These mutations produce either a reduced ability of tau to bind to microtubules, or an overproduction of 4 repeat tau isoforms, which leads in turn to the

assembly of tau into filaments similar or identical to those found in Alzheimer's disease brain *(19).* Phosphorylation, cleavage and conformational changes in tau protein play an important role in AD, the conformational changes and truncation of tau occuring after the phosphorylation of tau *(20).*

### 1.2.2 Clinical symptoms and diagnosis

In 1906, the German neuropathologist and psychiatrist Alois Alzheimer (1864-1915) gave a lecture in which he described for the first time the clinical symptoms and the neuropathological features now known as Alzheimer's disease.

Nowadays, the Board of Directors of the American Association for Geriatric Psychiatry adopted the following definitions:

**Alzheimer's disease** is a specific degenerative brain disease characterized by senile plaques, neuritic tangles, and progressive neuronal loss; also, the presumptive cause of AD.

**Dementia Resulting From Alzheimer's Disease** is characterized by decline primarily in cortical aspects of cognition and following a characteristic time course of gradual onset and progression *(21).*

Clinically, AD starts with occasional episodic memory deficits (like difficulties in recalling recent events of daily life), deficits in verbal functions, attention, visuospatial abilities and executive functions. The sensory-motor performance seems to be intact *(22).*

As the disorder progresses, cognitive decline get from unifunctional to global deficits, but functions coordinated from medial and lateral temporal lobes (episodic and semantic memory, respectively) are more affected than those coordinated from the frontal lobes *(23).*

Neuropsychiatric symptoms like aggression/agitation, depression, delusions, apathy, anxiety or hallucinations are other prominent features of AD, which may increase in frequency and intensity with declining cognitive function or may simply be correlated with duration of disease *(24).* The abuse of Antipsychotic

medications, for the treatment of neuropshychiatric symptoms accelerates the cognitive decline.

Dysfunction of the motor system will resemble extrapyramidal motor disorders. Thus, in the latest stage, in average 7-10 years after the onset, patients become immobile and die of minor respiratory difficulties such as aspiration or pneumonia *(25).*

Although there are no definitive imaging or laboratory tests except for brain biopsy, for diagnosis a combination of clinical history, physical, neurological and pshychitric examination, neuropsychological performance testing, laboratory evaluation and other diagnostic tests (like neuroimaging) are used to assess the disease *(21, 26).* The biochemical markers such as cerebrospinal fluid protein tau, beta-amyloid-42 peptide and neural thread protein are relevant to the pathology of AD and helps ruling out other causes of dementia.

The PET tracer $^{11}$C-labeled Pittsburgh Compound-B ($^{11}$C-PIB) also known as N-methyl[11C]2-(4'-methylaminophenyl)-6-hydroxy-benzothiazole is used to detect amyloid deposition in vivo. In AD patients, there is a high PIB retention particularly evident in the frontal, parieto-temporal, and posterior cingulate cortices, brain areas known to have many amyloid plaques *(27),* (Fig. 2).

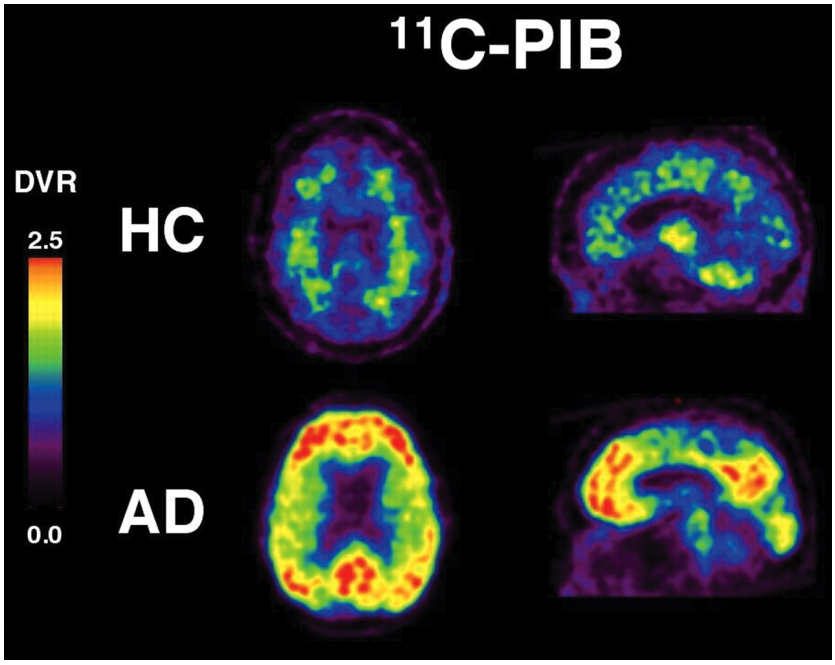


**Fig. 2.** $^{11}$C-PIB PET scans displayed in axial and sagittal plane from two representative subjects: a 84-year-old healthy control (HC) subjec, and a 83-year-old Alzheimer's

disease patient (AD) *(27).*

### 1.2.3 Neuropathological features

Alois Alzheimer published in 1911 an article “Über eigenartige Krankheitsfälle des späteren Alters” where he made for the first time a review of the histopathological spectrum of AD raging from “plaque only” to “tangles and plaques” *(28).*

The pathological hallmarks of the disease include extracellular deposits of beta-amyloid peptide (Aß) (Fig. 3A), intracellular neurofibrillary tangles (NFTs) (Fig. 3B), neuronal degeneration and synapse loss together with an inflammatory response and the depletion of the cholinergic system.

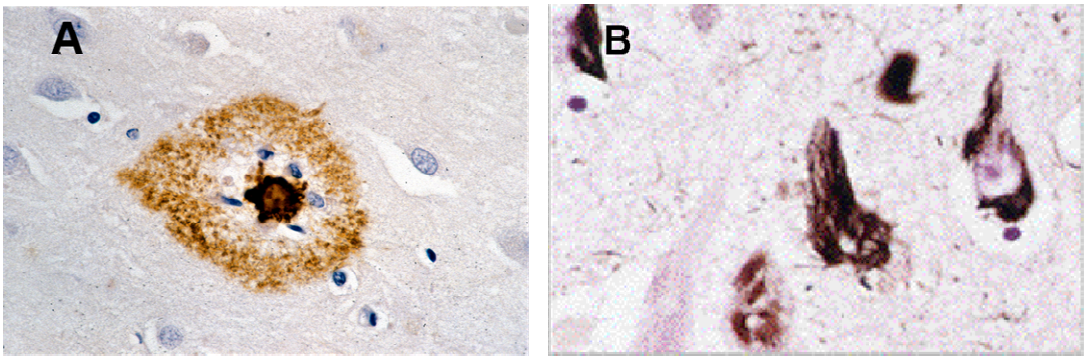


**Fig. 3.** The neuropathological features of AD: Amyloid plaque (A) and neurofibrillary tangles (surrounding a neuritic plaque) (B) in an AD brain (pictures generously provided by M. Tolnay from Department of Neuropathology, Institute of Pathology, University of Basel)

#### 1.2.3.1 ß-Amyloid-plaques

Senile or neuritic plaques are composed of abnormal extracellular deposits of amyloid-ß peptide that include abundant insoluble amyloid fibrils intermixed with nonfibrillar forms of the peptide. They are surrounded by dystrophic dendrites and axons, activated microglia and reactive astrocytes *(29).* Aß derives from amyloid precursor protein. Cerebral amyloidosis occurs predominantly in the neocortex and the hippocampus.

More frequently, the senile plaques probably start with an amorphous aggregation of Aß (mainly Aβ42 species with little or no Aβ40), and lack neuritic dystrophy and glial changes. They have been described not only in brain-regions like striatum, thalamus and cerebellum of AD patients, that are usually not involved in the clinical syndrome, but also in normal ageing individuals. After a while this "difuse" plaques become increasingly fibrillar (containing compact fibrils 7-10 nm), which can be stained with Congo red or thioflavin (that bind amyloid) *(30).*

This dense-core structures or mature amyloid plaques are often associated with numerous dystrophic neuritis and contain as well reactive microglial cells, which aggregate near the amyloid core, and activated astrocytes situated more at the periphery of the plaques *(31).* The presence of a high number of such compacted plaques in limbic and association cortex by the neuropathological examination remains the definitive diagnostic of Alzheimer's disease *(30).*

Besides diffuse and compact plaques, Aβ can also be deposit in cortical and meningeal arteries, arterioles, capillaries and, less often venules, of till 80% AD patients *(32).* This cerebral amyloid angiopathy (CAA) affects the integrity of the vessel walls and can cause cerebral hemorrhages.

Amyloid beta peptide is a small fragment of the amyloid precursor protein processed by three proteases: alpha, beta, and gamma *(33).* Aß mainly occurs in different lengths: Aβ1-40, Aβ1-42, the last one being highly amyloidogenic. APP is a type-I integral transmembrane glycoprotein, ubiquitously expressed and whose function has not been identified yet *(34).*

Most APP is normally guided through the nonamyloidogenic processing, alfa secretase cleaving within the Aß region. Alternatively, the cleavage by beta-secretase (BACE = β-site APP-cleaving enzyme) corresponds to the amyloidogenic pathway and represents the first step in the generating Aß. The final enzymatic step is performed by gamma-secretase complex, composed of 4 subunits: presenilin 1 and 2 (PS1, PS2) -who form the active site-, nicastrin, anterior pharynx defective-1 (Aph-1), and presenilin enhancer-2 (Pen-2) *(35).* The cleavage occurs within the membrane and being not sequence specific generates a variety of Aß peptides, Aß40 and Aß 42 as the major species *(116).* Aß40 is the most common form but it has been showed that longer Aß foms

display a higher propensity for aggregation and fibrillogenesis *(36),* so an increased Aß (particularly Aß42) production are responsible for enhanced deposition of Aß plaques.

### 1.2.3.2 Neurofibrillary tangles

NFTs are intraneuronal cytoplasmic bundles of paired helical filaments. They are composed of hyperphosphorylated isoforms of the microtubule-associated protein tau *(37),* which in normal cells promotes polymerization of tubulin monomers into microtubules, components of the intracellular transport system *(38),* and is essential for axonal growth and development *(39).*

Tau confers the microtubule stabilization but also flexibility as needed. Because of the hyperphosphorylation by many of the protein kinases, such as glycogen synthase kinase-3 (GSK-3), cyclin-dependent kinase 5 (CDK5), and the microtubule-affinity-regulating kinase (MARK), tau affinity to microtubules is reduced. The precise roles of the two forms of GSK-3, alfa and beta, are unknown *(40).*

NFTs are not specific to Alzheimer's disease, being found in other neurodegenerative diseases too, like in hereditary frontotemporal dementia and parkinsonism linked to chromosome 17 (FTDP-17). Mutations of the tau protein produce several changes including an alteration in the ratios of 4R/3R tau (isoforms containing either four or three microtubule-binding repeats). These cause tau hyperphosphorylation *(41)* and microtubule destabilization, which hinder axonal transport and produce inappropriate protein metabolism, synaptic malfunction and impaired signaling by retrograde neurotrophic factors *(42).* This can lead to the degeneration of dendrites and a loss of synapses at their axonal projection targets and to neuronal death. Another causes of tau abnormalities are mutations in APP, PS1 or PS2, which result in an increased amount of Aß peptide *(41),* (Fig. 4). However, the mechanisms that link senile plaques and NFTs have not yet been fully established *(43).*

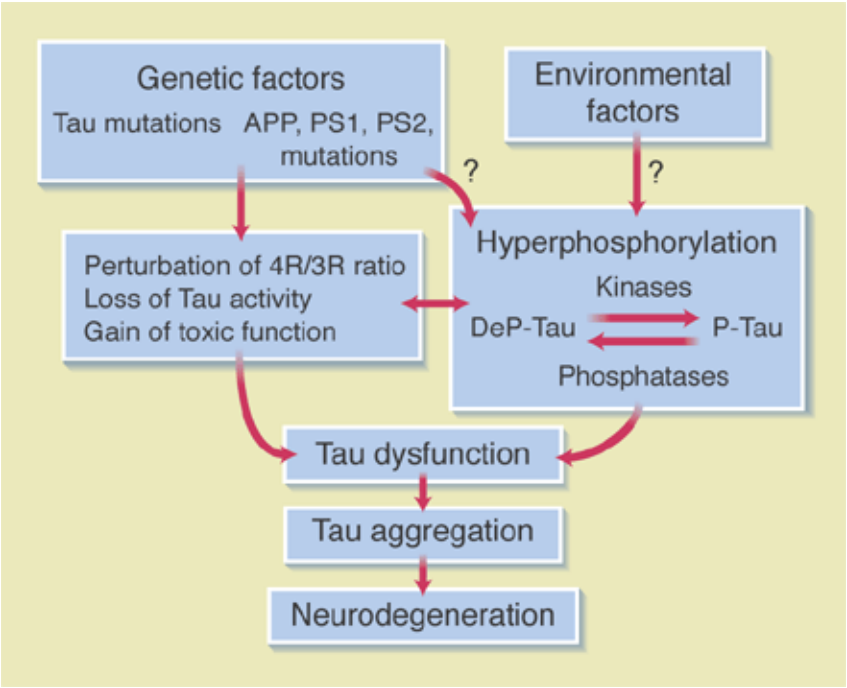


**Fig. 4.** Causes of tau malfunction and implicitly neurodegeneration, and their interconnection *(41).*

NFTs are first observed in the pre-α layer of the transentorhinal region, (stages I and II of the Braak classification), causing no cognitive impairment. In the stages III and IV the limbic system is affected, and in the stages V and VI the entire cerebral cortex and neocortical association areas are severely destroyed and the patients meet the neuropathological criteria for the diagnosis of AD (*44).* In addition neuronal loss in the nuclei of major neurotransmitter pathways is important, the death of cholinergic, adrenergic, serotonergic and dopaminergic neurons leading to deficit in acetylcholine, norepinephrine, serotonin, respectively dopamine *(45).*

### 1.2.4 Amyloid cascade hypothesis?

In 1991 John Hardy and David Allsop proposed The Amyloid Cascade Hypothesis, which suggests that the mismetabolism of APP and Aß deposition are the primary events in AD pathogenesis *(46).* According to this, the

imbalance between Aß production and Aß clearance followed by its deposition triggers a series of processes including synaptic dysfunction, microgliosis and neuronal loss.

However while between the distribution and density of Aß deposits and the severity of dementia is a low correlation, a good correlation seems to be between the synaptic loss and the dementia *(47).*

The patients with frontotemporal dementia (FTDP-17) present neurofibrillary tangles in the absence of amyloid deposits proving that tau abnormalities are sufficient to cause neuronal loss *(47).*

The toxicity of Aß depends on its aggregation state, the best correlation with the degree of cognitive decline occuring with soluble levels of Aβ (biochemically measured) *(48).* Aß is neurotoxic by inducing a number of possible mechanisms such as oxidative stress, excitotoxicity, disruption of mitochondrial function, induction of apoptotic genes through inhibition of Wnt *(49),* energy depletion, inflammatory response and apoptosis. But the exact mechanism by which Aß produce synaptic loss and neuronal death is controversial *(50).*

However, it has been observed that NFTs formation increases in cell bodies whose axons terminate in regions containing Aß bearing neuritic plaques in transgenic mice expressing both mutant APP and mutant tau, compared with transgenic animals expressing only mutant tau *(51, 52).* This suggests that extracellular accumulation of Aβ promotes the intracellular tau filament assembly *in vivo*.

According to Terwel D. et al, it seems that amyloid induces tauopathy through activation of GSK-3 ß (glycogen synthase kinase β), which increases tau phosphorylation, and leads to cell death *(53).* Beside this, (GSK-3) regulates catein phosphorylation (that can bind presenilin-1) and the cleavage of APP carboxy-terminal *(54),* interfering therefore with the generation of both amyloid plaques and tangles in Alzheimer's disease *(55),* (Fig. 5).

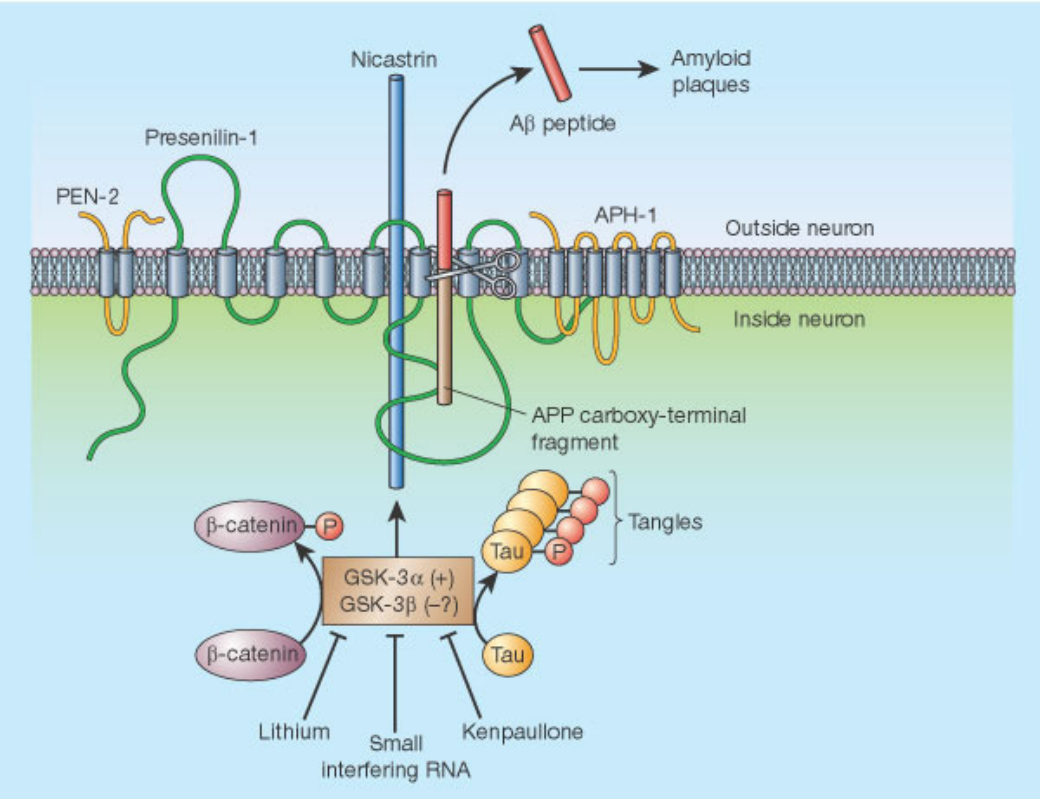


**Fig. 5.** Amyloid plaques contain Aß peptide, which is produced from the proteolityc processing of APP by α-, β- and γ-secretase *(55).* Glycogen synthase kinase-3 (GSK-3) regulates tau and catein phosphorylation (the last one can bind presenilin-1), and the cleavage of APP carboxy-terminal *(54).* The inhibition of GSK-3 by lithium and kenpaullone and its down-regulation by small interfering RNAs hinder Aß production *(55).*

Yet, despite intensive interest, the exact mechanistic relationship between the formations of neurofibrillary tangles, amyloid plaques, vascular amyloid and neurodegeneration observed in the AD brain remains still little understood.

### 1.2.5 Therapeutic approaches

At present, no treatments have been proved to stop or reverse the disease process, and therapy remains confined to symptomatic palliative interventions *(47).*

Degeneration of cholinergic neurons in AD leads to deficits in the choline acetyltransferase, responsible for the neurotransmitter acetylcholine

synthesis. Cholinesterase inhibitors block the degradation of acetylcholine *(56)* and offer some symptomatic relief. Drugs from this class, already on the market, are: donepezil (Aricept), galantamine (Razadyne), rivastigmine (Exelon), and tacrine (Cognex). N-methyl-D-aspartate (NMDA) is a receptor antagonist memantine (Namenda), who targets the glutamatergic neurotransmitter systems *(57)*. Unfortunately, these drugs induce a series of adverse reactions and have a modest effect on cognitive functions and on behavior.

Some potential neuroprotective strategies that are seeking to target biochemical stressors, such as inflammation, oxidation, and the disruption of hormonal processes (implicated in the neuronal loss from AD) might have therapeutic potential *(58).*

Inhibiting the cyclooxygenase, and therefore reducing the inflammatory response, NSAIDs have been investigated for their potential to delay the onset and slow the progression of AD *(59).* Besides an anti-inflammatory action, some NSAIDs can modify gamma-secretase activity, an effect that is independent of the drugs' inhibition of cyclooxygenase and other inflammatory mediators *(60).*

Antioxidants, like vitamins A, C, and E, coenzyme Q, and selenium have been suggested to reduce the risk of AD *(61).*

Because APP processing and Aß production are sensitive to cholesterol levels *(62),* treatment with cholesterol lowering drugs like statins, reduces serum Aß concentration in a dose-dependent manner *(63).*

Although Aß as well as tau protein seems to play central roles in the neuropathology of Alzheimer's disease, most of the industry's efforts have been focused on the 'amyloid hypothesis' and associated targets *(57).* Therapeutic attention has concentrated on developing inhibitors of either beta- or gamma-secretase, and/or stimulators of alpha-secretase to reduce Aß production, on blocking Aß aggregation into plaques, on lowering its levels in the brain, and on disassembling the existing amyloid plaques *(57).*

Being shown that the toxicity of Aß depends on its aggregation state *(64),* finding chemical agents that directly target Aß and its varied conformations, as well as inhibitors of Aß oligomerisation should prevail against those that merely block Aß deposition *(50).*

Pasive immunization with anti-Aβ antibodies *(65, 66),* or active immunization

with Aβ peptide *(67, 68)* not only prevented amyloid deposition in young mice but also cleared plaques and reduced associated glial and neuronal cytopathology in older animals. Based on these results, Elan Corporation moved into clinical trials with the active Aβ-vaccination approach, but the Phase II trial, was suspended in January 2002, when 6% of the patients developed clinical signs of meningoencephalitis *(69, 70, 71).*

Therapeutic strategies targeting tau are based on the identification of drugs that inhibit one or more tau kinase(s) and the tau fibril formation, dissolute the pre-existingaggregates activate the chaperone systems or stabilize the MTs. (Table 1)

**Table 1.** Therapeutic strategies targeting tau *(adapted from 43).*

| Therapeutic approach | Expected effect | Current status |
|---|---|---|
| Kinase inhibition | Prevent the abnormal phosphorylation rate or state of tau and consequent excessive disengagement of tau from the MTs | Various stages of preclinical investigation |
| Inhibition of tau fibril formation or dissolution of pre-existing aggregates | Prevent aberrantly phosphorylated and/or misfolded tau from forming more organized aggregates | Early stages of drug discovery |
| Activation of chaperone systems | Facilitate the clearance of misfolded tau and/or tau aggregates | Early stages of preclinical investigation |
| Stabilization of the MTs | Compensate for the loss of tau's MT-stabilizing function, and thereby sustain axonal transport | Different programmes are at various stages of development, ranging from preclinical investigations to Phase II studies |

Incomplete mouse models that recapitulate only specific aspects of AD pathogenesis have been key to the development of Aβ42-targeted therapies, as well as to the current understanding of the interrelationship between cerebral β-amyloidosis and tau neurofibrillary lesions. They are currently also used to develop novel diagnostic agents for in vivo imaging *(70).*

Stem-cell therapy and gene-replacing therapy remain experimental and far from clinical application.

### 1.2.6 Transgenic mouse models of Alzheimer's Disease

Parts of this and following chapter have been published in the paper: Radde R, **Duma C**, Goedert M, Jucker M: *The value of incomplete mouse models of Alzheimer's disease*, Eur J Nucl Med Mol Imaging, 2008 *(72).*

A variety of transgenic mouse models have been generated to study Alzheimer's disease (AD) pathogenesis (http://www.alzforum.org/res/com/tra/default.asp). The cascade of AD associated pathologies in most mouse models is triggered by the overexpression of the amyloid precursor protein (APP) carrying mutations which cause autosomal-dominant inheritable forms of familial AD (FAD) in humans *(73).* These mutations alter the proteolysis of APP to Aβ by affecting the affinities of the cleaving enzymes BACE1 and γ-secretase to its substrate. Mutations in the catalytic subunit of the γ-secretase complexes, presenilin1 (PS1) and presenilin2 (PS2), can also lead to FAD. The majority of the PS1/2 mutations shift the ratio of Aβ42/40 towards Aβ42, either through a reduction of Aβ40 generation or by increasing production of the more fibrillogenic Aβ42 *(74, 75)*. Both Aβ species are the main components of the amyloid deposits, major hallmark pathology of AD (Fig. 6).
The transgenic mouse models that overexpress mutated human APP with or without additional expression of mutated PS1/ 2 display a wide range of parenchymal and vascular amyloid deposits *(76).* These lesions are overall similar to those seen in AD brain, although biochemical differences in the deposited Aβ (e.g. posttranslational modifications) exist between mouse models and AD brain *(77, 78).* Some models develop predominantly neuritic plaques, while others exhibit diffuse plaques to a greater extent *(79, 80).* Neuritic plaques are accompanied by dystrophic neurites, reactive astrocytes, and hypertrophic microglia, and exhibit defined sites of neurodegeneration with severe synaptic pathology and focal loss of neurons *(81-83)* In contrast to the AD brain where substantial neuronal loss in hippocampus and specific neocortical regions is observed *(84, 85),* in most transgenic mouse models, no "global" neuron loss is observed *(86, 87).* Only in mice severely affected with neuritic plaques, a region-specific neuron loss, which correlates to amyloid burden, has been

reported *(88).*

Abnormal (murine) tau phosphorylation patterns are observed in APP and APP/PS transgenic mice within dystrophic neurites in the vicinity of amyloid deposits *(79, 89, 90).* However, no typical flame-shaped NFTs are observed in mice that carry FAD mutated human APP or mutated PS1/2. NFT formation in mice can be induced by the overexpression of tau constructs that carry familial

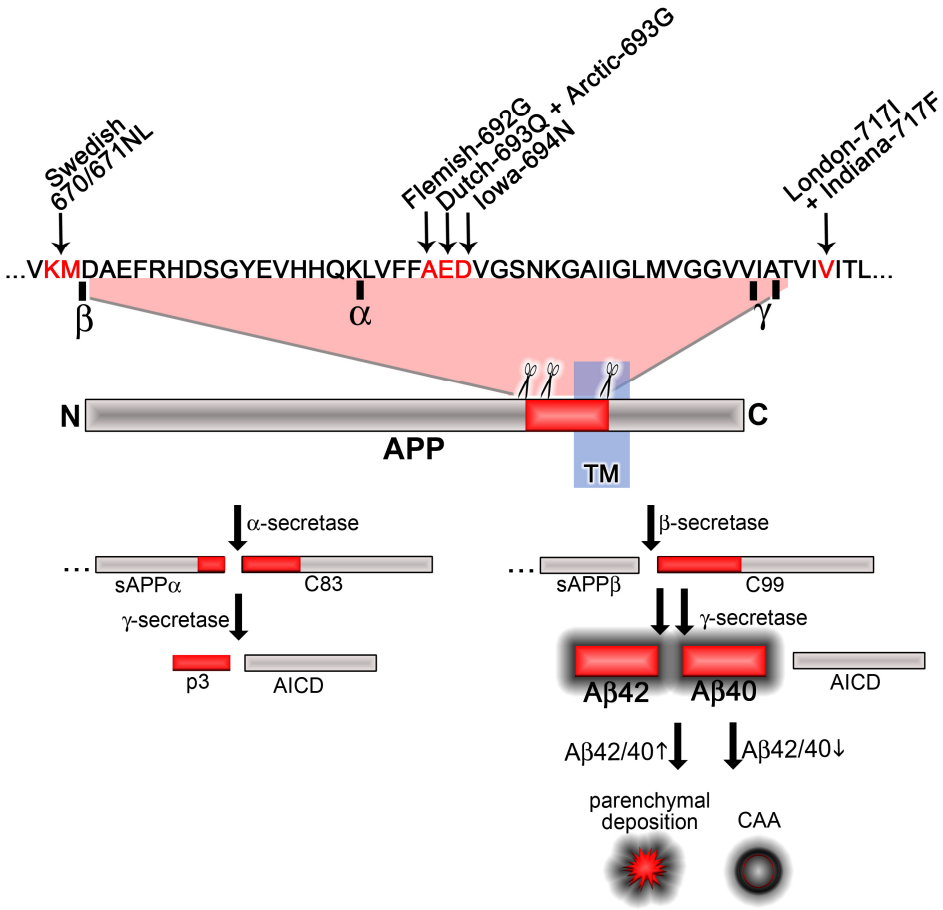


**Fig. 6.** APP processing and APP mutations used to generate transgenic mouse models of AD. FAD mutations, positions and substitutions of amino acid residues in commonly used transgenic mice are shown above the APP sequence. The cleavage sites for α-, β- and γ-secretase are indicated within the sequence (α, β, γ) and i n the schemat ic drawi ng of full l ength APP (scissors). The transmembrane (TM) region is indicated in blue. Non-amyloidogenic proteolysis of APP by α-secretase cleaves the Aβ peptide, thereby releasing the soluble sAPPα. Subsequent γ-secretase cleavage of C83 results in p3 production and AICD. The alternative amyloidogenic proteolysis of APP by the β-secretase produces soluble sAPPβ. This is followed by proteolysis of C99, which is

subsequently heterogeneously cleaved by γ-secretase, which results in AICD and Aβ generation of various lengths (Aβ40 vs. Aβ42). The production of low Aβ42/40 ratios yields predominant CAA, while high Aβ42/40 ratios direct amyloid deposition into brain parenchyma *(72).*

mutations found in frontotemporal dementias *(91–93).* Apart from the fact that these tau lesions consist of mutant tau, NFTs in mice appear similar to those observed in AD brain *(94).*

To mimic the spatial and temporal expression of APP in human brain, genomic-based yeast artificial chromosome transgenic mouse models have been developed *(95).* While the value of such models is more closely paralleling expression of the human gene, it was the more experimental cDNA-based mouse models with cell- and region-specific APP expression that have led to mechanistic insights into AD pathogenesis. For example, the overexpression of APP with neuron-specific promoters has unequivocally demonstrated that neuronal expression of APP is sufficient to induce both parenchymal and vascular amyloid-related pathology *(96).*

Cerebral amyloid angiopathy (CAA) can be found in nearly every brain of sporadic and familial AD. Thus, the contribution of parenchymal amyloid (or the development thereof) vs. vascular amyloid to the cognitive impairment and pathological cascade of AD is of great importance. Thereby, not only mouse models that recapitulate the situation in the AD brain are needed, but also mouse models that either develop only CAA or only parenchymal amyloid. It is known that the ratio of Aβ42/40 determines the sites of amyloid deposition, i.e. Aβ40 over Aβ42 results in predominant vascular amyloid, while a shift towards Aβ42 results in amyloid deposition in the parenchyma *(97).* Thus, APP transgenic mice were recently generated that additionally express L166P mutated PS1, because this, mutation results in an extremely high Aβ42/40 ratio. As predicted, the resulting APPPS1 transgenic mice develop robust neuritic amyloid plaques with only negligible CAA *(90).*

The observation that APP and/or APP/PS overexpressing mouse models do not develop NFTs was initially seen as a disappointment. Nevertheless, the mechanistic interplay between Aβ and tau has been convincingly demonstrated

by the cross-breeding of mice overexpressing mutant tau with mice over-expressing mutant APP *(51, 98, 99).* Thus, the combined APP and tau overexpression has led to mouse models that mimic the two hallmarks of the AD brain: cerebral amyloidosis and NFTs.

### 1.2.7 The aim of this study

To study Alzheimer's disease (AD), a variety of mouse models has been generated through the overexpression of the APP and/or the presenilins harboring one or several mutations found in familial AD. Mouse models that recapitulate only specific aspects of AD pathogenesis are of great advantage when deciphering the complexity of the disease and can contribute substantially to diagnostic and therapeutic innovations.

Most of the commonly used transgenic mouse models express both murine and human Aβ, and co-deposition of mouse Aβ in addition to the transgene-derived human Aβ occurs to various degrees. Such a co-deposition of amyloid from different species does not occur in AD brain and can be avoided by the use of knock-in mice or by backcrossing transgenic mice to an App-null background.

Lack of NFTs and missing neuron loss are the most obvious difference in pathology between APP, APP/PS transgenic mouse models and the AD brain. This observation shows that mutated human APP and/or PS1/2 overexpression is not sufficient to induce the entire pathological cascade in mice. Identifying the additional factors that trigger a more complete AD phenotype in mice is desirable *(72).*

The objective of the present work was to study the potential amyloid interfering effect of murine Aß on human Aß deposition. Moreover, the interaction between Aß deposits and tau lesions has been investigated.

# 2. Material and Methods

## 2.1 Material

**Tab. 2. Buffer and solutions**

| Buffer and solutions | Company |
|---|---|
| Homogenation Buffer | 0.6055 g 50mM Tris pH 8<br>0.8706 g 150mM NaCl<br>0.1861 g 5mM EDTA<br>bring to 100 ml with ddH2O<br>add 10 Mini Complete protease inhibitor tablets |
| **Wiltfang stock solutions and buffers:** | |
| 4x Separation Gel Buffer (1.6 M Tris-base, 0.4M H2SO4) | 19.38 g Tris-base<br>80 ml ddH2O<br>adjust to pH 8.4 with approximately 8ml 5M H2SO4<br>bring to 100 ml with ddH2O |
| 2x Stacking Gel Buffer (0.8M Bis-Tris, 0.2M H2SO4) | 16.7 g Bis-Tris<br>80 ml ddH2O<br>adjust to pH 6.7 with approx. 4ml 5M H2SO4<br>bring to 100 ml with ddH2O |
| 2x Comb Gel Buffer (0.72M Bis-Tris, 0.32M Bicine) | 3.77 g Bis-Tris<br>1.3 g Bicine<br>bring to 25 ml with ddH2O |
| 2x Wiltfang Sample Buffer | 1.5 g Bis-Tris 718mM<br>0.519 g Bicine 318mM<br>2 ml 10% SDS 2%<br>3 g Sucrose 30%<br>500 µl 2-Mercaptoethanol 5%<br>400 µg Bromphenolblue 0.008%<br>bring to 10 ml with ddH2O |
| 1x Cathode Buffer (ph 8.2; 0.2M Bicine, 0.1M NaOH, 0.25% SDS) | 32.64 g Bicine<br>800 ml ddH2O<br>adjust to pH 8.2 with approx. 90 ml 1M NaOH<br>add 12.5 ml 20% SDS and bring to 1000ml with ddH20 |

| | |
|---|---|
| 1x Anode Buffer (pH 8.1; 0.2M Tris-base, 0.05M H2SO4) | 24.22 g Tris-base<br>900 ml ddH2O<br>adjust to pH 8.1 with approx. 10 ml 5M H2SO4<br>bring to 1000 ml with ddH2O |
| Separation Gel | 4.8 g Urea<br>2.5 ml 4x Separation Buffer<br>3.3 ml Acrylamide 30%<br>bring to 10 ml with ddH2O<br>add 100 µl 10% APS and 5 µl TEMED |
| Stacking Gel | 1 ml 2x Stacking Gel Buffer<br>562 µl ddH2O<br>400 µl Acrylamide 30%<br>20 µl 10% SDS<br>add 16 µl APS 10% and 2 µl TEMED |
| Comb Gel | 1.5 ml 2x Comb Gel Buffer<br>750 µl Acrylamide 30%<br>705 µl ddH2O<br>30 µl SDS 10%<br>add 12 µl APS 10 % and 3 µl TEMED |
| **Tris-Glycine stock solutions and buffers:** | |
| 2x Stacking Gel Buffer | 125 ml Tris-Cl ph 6.8<br>5 ml SDS 20%<br>bring to 500ml with ddH2O |
| 5x Resolving Gel Buffer | 112.62 g Tris-Cl ph 8.8<br>6.125 ml SDS 20%<br>bring to 500ml with ddH2O |
| 10x Running Gel Buffer | 72 g Glycine<br>315 g Tris<br>25 ml SDS 20%<br>bring to 500ml with ddH2O |
| Transfer buffer for nitrocellulose membranes | 14.41 g Glycine<br>3.0275 g Tris<br>200 ml Methanol 100%<br>bring to 1000ml with ddH2O |
| 3x Lämmli loading buffer | 2.4 ml Tris-Cl ph 6.8<br>3 ml SDS 20%<br>3ml Glycerine 100%<br>0.006 g Bromphenol blue<br>1.6 ml ß-mercaptoethanol |
| Resolving gel 8% | 3.2 ml acrylamide 30%<br>2.4 ml 5x Resolving Gel Buffer<br>5.5 ml ddH2O<br>add 100 ml APS 10% and 25 ml TEMED |

| | |
|---|---|
| Stacking gel 4% | 0.66 ml 30% Acrylamide<br>2.5 ml 2x Gelpuffer<br>1.8 ml ddH2O<br>add 50 µl APS 10% and 10 µl TEMED |

## 2.2 Methods

### 2.2.1 Generating of transgenic mice

For most experiments, APPPS1 transgenic mice were used, mice generated by coinjection of Thy1-APPKM670/671NL and Thy1-PS1L166P constructs into male pronuclei of C57BL/6J oocytes *(90)*. This double transgenic mouse line is a model of parenchymal amyloidosis, with an early onset in neocortex (at 2 months of age). In the hippocampus, amyloid deposits develop later (at 3-4 months of age). There is, at least in young mice, no gender effects in Aß level and amyloid deposition. The mice do not model the tau pathology and robust neurodegenaration noted in AD.
The APPPS1 mice were maintained on a pure C57BL/6 background and compared with APPPS1 mice on an APP null background *(96).*
In addition, heterozygous mice that expresses in nerve cells four-repeat human tau protein with the P301S mutation *(93)* were used. They exhibit the essential features of a human tauopathy, like the formation of abundant filaments made of hyperphosphorylated tau protein and nerve cell degeneration. The P301S transgenic mice were crossbred with APPPS1 transgenic mice, the littermate females being used for the study.
Mice were group housed in pathogen-free conditions. All procedures were in accordance with an animal protocol approved by the University of Tübingen and the government of Baden-Württemberg.

### 2.2.2 Genotyping of tail biopsies

DNA from tail biopsies was prepared using the DNeasy tissue kit (Qiagen). 0,4

to 0,6 cm of the mouse tail was incubated in 180µl Buffer ATL + 20µl proteinase K at 56°C overnight in a thermomixer. To the tissue lysate, 200µl Buffer AL and 200µl ethanol (96-100%) was added mixed thoroughly by vortexing several times. The mixture was transferred into a new tube (DNeasy Mini spin column in a 2ml collection tube) and centrifuged at 8000 rpm at room temperature for 1 min. The procedure was repeated, first with 500µl Buffer AW1 at 8000 rpm for 1 min and then with 500µl Buffer AW2 at 15000 rpm for 3 min. Finally, to the spin column in a new 2 ml collection tube, was added for elution 200µl Buffer AE, incubated for 1 min at room temperature and centrifuged for 1 min at 8000 rpm.
The following primer pairs were used:

☼ APPforward 5´-GAA TTC CGA CAT GAC TCA GG-3´, APPreverse 5´-GTT CTG CTG CAT CTT GGA CA-3´;

☼ hPS1forward 5´-CAG GTG CTA TAA GGT CAT CC-3´, hPS1reverse 5´-ATC ACA GCC AAG ATG AGC CA-3´ (the genotyping for APP was done routinely, while for PS1 only sporadically as a control because of the cointegration of the transgenes);

☼ ko-2forward 5'-CCA CGC AGG ATC ACG ATG-3', PGK-1reverse 5'-GAG TAG AAG GTG GCG CGA AG-3' ;

☼ ko-1forward 5'-CAA CCG AGG AGC TTG AAT CT-3', ko-1reverse 5'-TCT GCG TTC AAG GCT CGT CC-3'

☼ P301Sforward 5'-GGT TTT TGC TGG AAT CCT GG-3', P301Sreverse 5'-GGA GTT CGA AGT GAT GGA AG-3'

PCR program for APP and PS1 were performed as follows: 4 min 95°C; 45 sec 95°C; 45 sec 58°C; 45 sec 72°C; 5 min 72°C, hold at 4°C. Steps 2 to 4 were repeated 34 times.

PCR program for APPko: 3 min 95°C; 30 sec 94°C; 30 sec 55°C; 30 sec 72°C.Steps 2 to 4 were repeated 50 times.

PCR program for APPwt: 5 min 94°C; 45 sec 94°C; 45 sec 58°C; 45 sec 72 °C. Steps 2 to 4 were repeated 34 times.

PCR program for P301S: 5 min 94°C; 30 sec 94 °C; 30 sec 57°C; 45 sec 72°C. Steps 2 to 4 were repeated 34 times.

### 2.2.3 Histology and immunohistochemistry

APPPS1 mice on wild type C57BL/6 background and APPPS1 mice on an APP null background were anesthetized with 2.5% Isoflurane and decapitated. The cranium was cut away with small snips along the sides all the way forward to the snout and then the skullcap was removed. The brain was lifted and free from the vessels and cranial nerves.

The right hemispheres were immersion-fixed in 4% paraformaldehyde in PBS for 2 days, followed by incubation in 30% sucrose in PBS for 1 day. The hemibrains were subsequently frozen in 2-methylbutane and stored at -80°C until additional use.

40 µm thick coronal sections were cut with a freezing-sliding microtome and collected into cryoprotectant solution (30% ethylenglycol, 20% glycerol, 50 mM sodium phosphate buffer, pH 7.4).

The immunohistochemistry was done on free-floating sections, following the procedure published previously *(100).* Sections were rinsed in PBS for several times, incubated in 0.08% $H_2O_2$ in PBS, followed by incubation in PBS containing 0.3% Triton X-100 and 5% serum.

Primary antibody (like polyclonal anti-human Aß antibody DW6 -kindly provided by D. Walsh-; polyclonal antibody to ionized calcium binding adapter molecule 1 Iba1 -Wako, Richmond, USA-; murine Aß monoclonal antibody m3.2 - kindly provided by P. Mathews-; polyclonal antibody to glial fibrillary acidic protein GFAP –Dako-) was diluted in PBS with 2% serum and 0.3% Triton X-100, all in PBS and incubated at 4°C overnight. Sections were then incubated with biotinylated secondary IgG followed by the avidinbiotin-peroxidase complex solution (all from Vector Laboratories; Burlingame, CA). Congo red stainings were performed according to standard protocols.

The mice generated from the interbreeding of the two lines: APPPS1 and P301S, were injected intraperitoneally with Ketamine/Xylazine mix. The thoracic cavity was opened to access the heart. After ensuring that the sodium phosphate buffer (7.4) was flowing drop-wise and that no air bubbles were visible along the tubing, the cannula was inserted into the left ventricle and the right atrium was opened. The mice were perfused transcardially for 2 min with

PBS and 8-10 min with 4% paraformaldehyde in PBS.

The brains were then processed for paraffin embedding: they were kept overnight in 4% PFA in PBS, next day put into cassettes and an automated processor took them through a series of graded ethanol baths to dehydrate the tissues and then into xylene (http://www.fhcrc.org/science/labs/fero/). Hot paraffin permeated the tissues: 70% ethanol 30 min. (x1), 95% ethanol 30 min. (x2), 100% ethanol 30 min. (x2) xylene 30 min. (x2), paraffin (60°C) 30 min. (x1), paraffin (60°C) 30 min (x1) with vacuum.

Tissues processed into paraffin were melted by placing them in 65°C paraffin bath for 15 minutes. Block molds were warmed on a hot plate. Hot paraffin was poured into the mold and then the melted tissues were placed in the mold. To prevent the tissues from sticking, heated forceps were used. The mold was placed on a cooling plate when the tissue was in the desired orientation and the cassette backing was placed on top as a lid. After 15-20 minutes the hard paraffin blocks were popped out of the mold and the blocks were stored at room temperature.

Blocks to be sectioned were kept face down on an ice block for 5 minutes. A water bath was turn on 40°C and the block was fixed into the microtome so that the block faced the blade and was aligned in the vertical plane. Serial coronal sections were cut at a 5µm microtome setting. The slides with paraffin sections were placed in a 65°C oven for 30 minutes to bond the tissue to the glass.

The sections were deparaffinized in xylene 10 min followed by immersion in bath of decreased concentrations of ethanol, rinsed in PBS and then placed in Antigen Retrieval (MW-citrate buffer) for 35 min at 90°C. Sections were rinsed in PBS and incubated for 1 h in 5% goat serum. Slides were transferred to a humid chamber, and section were incubated overnight at 4°C with a monoclonal AT8 antibody (Innogenetics), diluted 1:1000 in PBS with 3% goat serum) specific to tau phosphorylated at ser-202 and thr-205.

They were then incubated for 30 min with biotinylated goat anti-rabbit IgG (obtained from Vector Laboratories, Vectastain ABC kits) diluted 1:200 in PBS with 3% goat serum, followed by incubation for 30 min in an avidin-biotin-peroxidase complex (Vector Laboratories) diluted 1:200 in PBS. Sections were reacted with 3,3'-diaminobenzidine (0.08%; Sigma, St. Louis, MO) and 0.03%

hydrogen peroxide in PBS for 2-3 min, rinsed, dehydrated, cleared, and coverslipped. In addition sections were stained hystologically with Congo red according to standard protocols and was used to assess compact amyloid *(101).*
MW-citrat buffer: 18ml A+ 82ml B + 900 dist H20, ph 6.0

A: 21.01g Citric Acid (C6H8O7xH2O) in 1000mll dist H20

B: 29.41g Trisodium citrate (C6H5Na3O7xH2O) in 1000ml dist H2O

### 2.2.4 Stereology

The burden of Aß deposition was quantified on random sets of every 12$^{th}$ systematically sampled DW6 immunostained coronal sections through the neocortex performed with the aid of Stereologer software and a motorized *x-y-z* stage coupled to a video-microscopy system (Systems Planning and Analysis, Inc., Alexandria, VA). The images were captured with an 20x objective and converted to 8-bit gray scale for calculating the percent area occupied by Aß immunoreactive pixels, performed using the public domain ImageJ. Results were statistically analyzed using ANOVA with the help of StatView 5.0.1. Both the mean and the SEM are indicated. The level of significance was set at $p < 0.05$ *(99).*

### 2.2.5 Plaque size determination

For the determination of plaque size one section per animal each from similar positions of the frontal cortex was imaged using the AxioFluor Mosaix Software (Zeiss, Jena). To identify individual plaques, ROIs, e.g. plaques were separated with the public domain software ImageJ and the watershed algorithm (http://bigwww.epfl.ch/sage/soft/watershed/) after application of Gaussian blurring ($\sigma = 5$). Cortices were traced and ROIs measured with ImageJ. Plaques were classified and statistically analyzed using StatView.

### 2.2.6 Electron microscopy

For comparative histochemical, immunofluorescence and immunogold staining,

serial thin sections were collected. Histological stains (with toluidine blue) were used in light microscopy to identify the orientation of the sample, and immunofluorescence to identify the plaques. Electron microscopy was used, for the subsequent sections labeled with immunogold, to identify amyloid fibrils at high resolution*(102).*

Mice were deeply anesthetized and perfused transcardially with 0.1M phosphate-buffered saline (PBS) followed by 4%PFA in PBS plus 0.1% glutaraldehyde. Brains were removed and postfixed overnight in 4% PFA in PBS.

The rest of the procedure, described below, has been done with the help of Dr. H. Schwarz, from Max Planck Institute for Developmental Biology, Tübingen, Germany. The next day the brains were sectioned on a vibratome and 150 µm slices were collected in 0.1 M PBS and dehydrated trough a graded series of increasing ethanol concentrations. Organic solvents dissolve and extract lipids and denaturate proteins in a temperature dependent manner; therefore the dehydration was performed by progressive lowering of temperature *(102).* The sections were then embedded in Lowicryl K11M and placed between 2 ACLAR films cut into a slide shape (200µm thick). Further pieces of brain tissue (neocortex) were removed with a scalpel and re-embeded in Durcupan blocks (Fluka, Steinheim, Germany). Using an ultramicrotome (Ultracut, Leica, Bensheim Germany) ultrathin sections (50 nm) were cut.

#### 2.2.6.1 Immunogold labeling

Grids with serial ultrathin sections were rinsed in PBG (0,2% gelatine in PBS plus 0.5% bovine serum albumin, BSA) at room temperature onto a clean parafilm surface for 10 min to mask nonspecific binding sites *(103).* The primary antibodies: NT12 (polyclonal anti-human Aß) and m3.2 (anti-murine Aß monoclonal) were diluted in the PBG 1:2000 and 1:1000 respectively. The sections were incubated 1h then rinsed in PBG.

NT12 and m3.2 were detected with 18 nm gold-coupled secondary goat-anti-rabbit antibody (Jackson) and 10 nm gold-coupled secondary goat-anti-mouse antibody (York), respectively. Sections were contrasted with 1% aqueous uranyl acetate for 3 min *(102)* and examined in a Philips CM 10 electron microscope.

### 2.2.6.2 Immunofluorescence labeling

The sections were collected from the water with Perfect Loop (Leica, Bensheim Germany) transferred onto round dry polylysine-coated coverslips and prevented from drying during the whole labeling procedure. The residual water was drained along the outside of the loop with a filter paper.

On coverslips the sections were encircle with a water-repellent silicon pen, were then placed in a humid chamber on parafilm with sections facing up and blocked with PBG for 10 min. PBG was aspirated with a pipette tip connected to a vacuum flask hooked to a vacuum pump and the sections were incubated with the first antibodies for 1h. The same antibodies concentrations as in immunogold labeling has been used.

The sections were washed with PBG, incubated with fluorochrome-labeled secondary antibodies (CY3, ALEXA 546) for 1h, washed again and then counter-stain nuclei for 5 min with DAPI. After a final wash with dist. water the coverslips were mount on glass slides using a drop of mounting medium (Mowiol) for fluorescence microscopy *(102).*

### 2.2.7 Biochemical analysis

For Elisa and western blot analysis frozen brain hemispheres lacking the cerebellum were added to 10 vol of 50 mM Tris, pH 8.0, 150 mM NaCl and 5 mM EDTA containing a proteinase inhibitor cocktail (Roche, Basel, Switzerland). They were first broken down mechanically using a homogenizer (Ika Ultra-Turrax) then sonicated with Labsonic M.

APP expression was analyzed using 8% Tris/glycin SDS-PAGE gels, while for Aβ analysis, SDS-PAGE with 10%T/5%C Bicine/Tris minigels containing 8M urea in the separation gel have been used *(97).* Synthetic Aß1-40 and 1-42 (Bachem, Bubendorf, Switzerland) were used as controls. The SDS-PAGE (sodium dodecyl sulfate polyacrylamide gel electrophoresis) allowed separation of proteins by their molecular weight, by maintaining the polypeptides in a denatured state once they have been treated with strong reducing agents to remove secondary and tertiary structure.

Sampled proteins, covered in the negatively charged SDS moved to the

positively charged electrode through the acrylamide mesh of the gel. The proteins were separated according to size (measured in kilodaltons), because smaller proteins migrate faster. The resolution of the gel is determined by the concentration of acrylamide - the greater the acrylamide concentration the better the resolution of lower molecular weight proteins and vice versa.

Proteins were transferred onto either nitrocellulose membrane or PVDF Immobilon-P membrane (Millipore, Eschborn, Germany), by semi-dry or wet blotting. The uniformity of transfer of protein from the gel to the membrane was checked by staining the membrane with Ponceau S dyes. To prevent the non-specific binding between the membrane and the antibody, the membrane was placed in a solution of powdered milk in PBS-Tween.

Human APP and Aβ were detected by monoclonal anti-Aβ 6E10 antibody, which recognizes amino acid residues 1–16 of Aß (diluted 1:2500). Murine Aβ and APP were detected with monoclonal m3.2 antibody, which recognizes an epitope within residues 11-15 of the rodent Aß sequence, a region that contains two amino acid differences when compared to the human sequence (diluted 1:1000). As an internal control polyclonal anti-α-tubulin antibody (Source) was used. The secondary antibody was horseradish peroxidase-conjugated goat anti-mouse IgG (Chemicon Temecula, CA). Bands were visualized using SuperSignal (Pierce, Rockford, IL) and exposed to Kodak X-OMAT AR film (Eastman-Kodak, Rochester, NY). Quantification of the signal (optical density) was done using the public domain software ImageJ (www.rsb.info.nih.gov/ij/).

Aß levels were determined by sandwich ELISA in the laboratories of Nathan S. Kline Institute for Psychiatric Research, New York, USA, by Assistant Professor P.M. Mathews, using the same brain homogenates as prepared for western blot analysis. Before ELISA experiments, Aß was extracted by formic acid *(97).* Aß carboxy-terminal monoclonal antibodies, which recognize exclusively either Aßx-40 (JRF/cAβ40/10) or Aβx-42 (JRF/cAβ42/26) were used for capturing Aß. Bound Aβ was detected with horseradish peroxidase-conjugated JRF/Aßtot/17 which recognizes the amino-terminal 16 residues of human Aß *(90).* The results are reported as the mean ± SEM in pmol Aβ per g wet brain, based on standard curves using synthetic Aβ1-40 and Aβ1-42 peptide standards (American Peptide

Co. Sunnyvale, CA).

### 2.2.8 PIB binding

The PIB[$^3$H] binding was done in the laboratories of the Department of Psychiatry at the University of Pittsburgh, USA, by Prof. W.E. Klunk, on brain homogenates. ~1 nM [H-3]PiB has been added to 100 mg/ml of brain homogenate in the presence and absence of excess cold PiB (1 µM).

### 2.2.9 Statistical analysis

Statistical analysis was performed using the StatView 5.0.1 Software. The results are expressed as mean values ± standard errors of the mean (SEM). Statistical significance is indicated as follows: *$p < 0.05$, **$p < 0.01$, and ***$p < 0.001$.

# 3. Results

## 3.1 Murine Aß interferes with human Aß

APPPS1 mice on a wild type C57BL/6 background have been compared with APPPS1 on an APP null background (thereafter referred to as wtAPPPS1 and koAPPPS1, respectively). koAPPPS1 mice are a transgenic mouse model without the expression of interfering endogenous mouse APP.

### 3.1.1 Co-integration of murine Aβ in amyloid plaques

Immunohistochemical analyses of brain tissue from 5-mo old males wtAPPPS1 and koAPPPS1 mice revealed co-deposition of murine with human Aβ in wtAPPPS1 mice, whereas no murine Aβ could be detected in brain of koAPPPS1 mice (Fig. 7B, A).
Murine APP expression was detected in wtAPPPS1 and wild type mice using the m3.2 antibody. Murine Aβ could only been shown in wtAPPPS1 mice, while in non-transgenic wild type animals murine Aβ was beyond detection level (Fig. 7C), indicating the accumulation of murine Aβ in amyloid plaques as proven by electron microscopy (immunogold labeling) (Fig. 7D,E), and by light microscopically analyses (fluorescence labeling) (Fig. 7F,G,H).

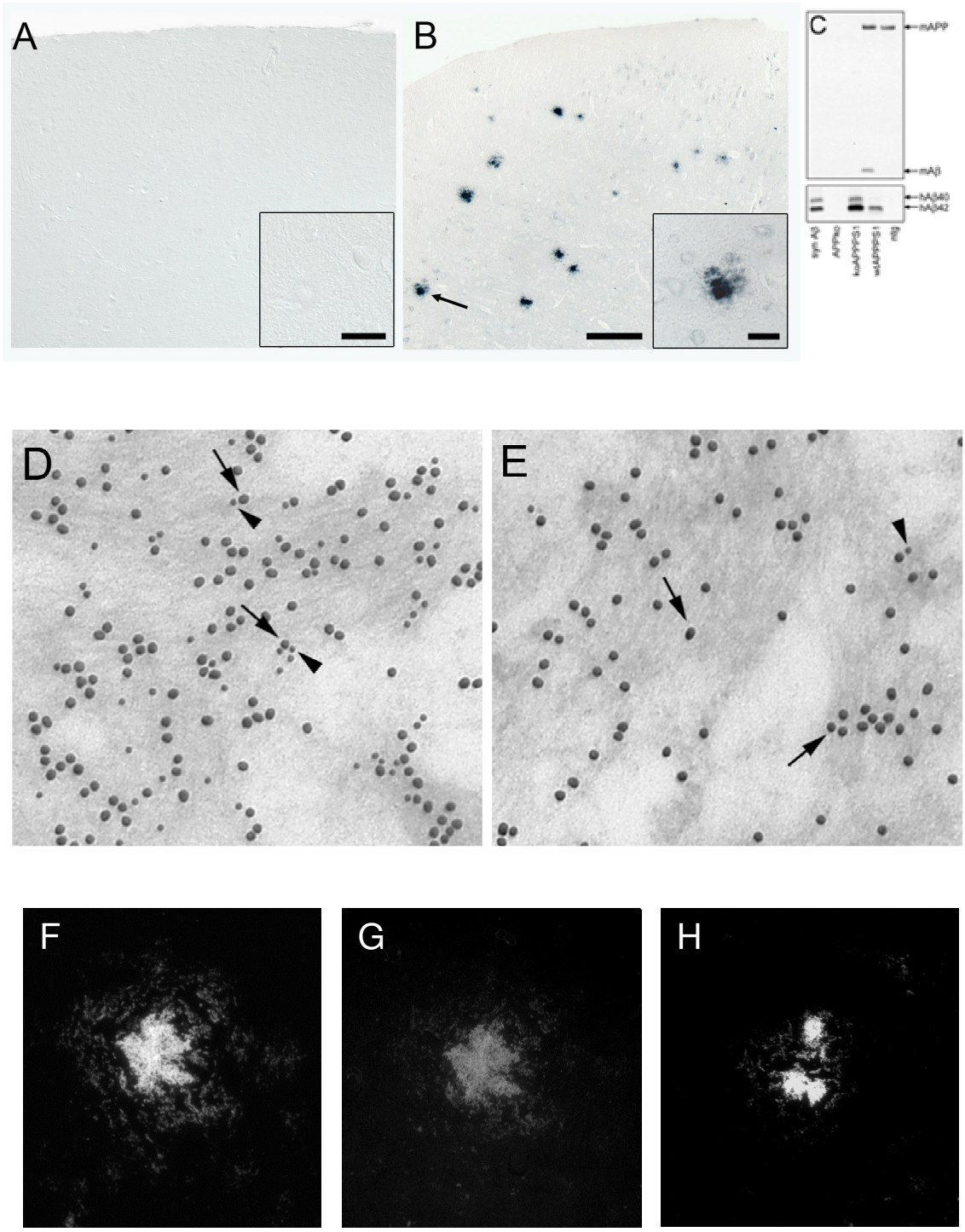


**Fig. 7.** Immunostaining with m3.2 antibody specific to murine Aβ shows no detectable labeling in 5-mo old koAPPPS1 male mice **(A)**. Sections from the frontal neocortex of 5-mo old wtAPPPS1 mice reveal the co-deposition of murine Aβ with human Aβ **(B)**. Insets are magnifications from arrow indicated areas of (A) and (B). Scale bars

represent 100 µm and 20 µm, respectively. Western blot analyses reveal murine APP expression in wtAPPPS1 and in non-transgenic wild type (ntg) mice (antibody m3.2). Murine Aβ was only detectable in wtAPPPS1 mice. Note the increased human Aβ40 and Aβ42 levels in koAPPPS1 mice, by using 6E10 Aß. Synthetic human Aβ (syn Aβ) was used as a molecular weight standard and ntg APPko mice as negative controls. Mice used for western blot analysis were 7-mo old males **(C)**. Electron micrograph reveals tight association of 10 nm gold-decorated murine Aβ (arrowheads) and 18 nm (arrows) gold-decorated human Aβ in the neocortex of a 14-mo old female wtAPPPS1 mice **(D)**. koAPPPS1 control sections exhibit hardly no murine Aβ, just faint background staining was detected **(E)**. wtAPPPS1 section labeled for human Aß and detected with Cy3 **(F)**, labeled for murine Aß and detected with Alexa 546 respectively **(G)**. Section of a koAPPPS1 mouse labeled for human Aß and detected with Cy3. Images were taken with a 40x objective **(H)**.

### 3.1.2. Subtle changes of amyloid deposition in wtAPPPS1 and koAPPPS1 mice

At 2 months of age amyloid plaques were present in the neocortex of both lines. At 7 months they covered the entire forebrain and in 14 months old wtAPPPS1 and koAPPPS1 mice they have been found in all brain regions (Fig. 8). The site of deposition and the onset of amyloidosis did not differ in koAPPPS1 and wtAPPPS1 mice.

At the age of 2 months when first deposits appear in both lines as dense congophilic aggregates, no differences in amyloid plaque structure were observed (Fig. 9A). In 7-months old mice when diffuse amyloid material assembles around the dense cored plaque, koAPPPS1 mice display in contrast to wtAPPPS1 mice larger individual plaques with looser structure (Fig. 9A).

Stereological analyses revealed almost equal amyloid burden in both APPPS1 transgenic mouse line at 2 and 7 mo of age (Fig. 9B), indicating that this method is not sensitive enough to detect subtle changes in plaque size and plaque conformation. Larger individual plaque size in 7-mo old wtAPPPS1 mice could be shown by direct quantification of individual plaque area (Fig. 9C,D). No alterations of the concomitant neuroinflammation could be observed with

immunostainings against the microglial marker protein Iba1 in koAPPPS1 mice (Fig. 9E,F).

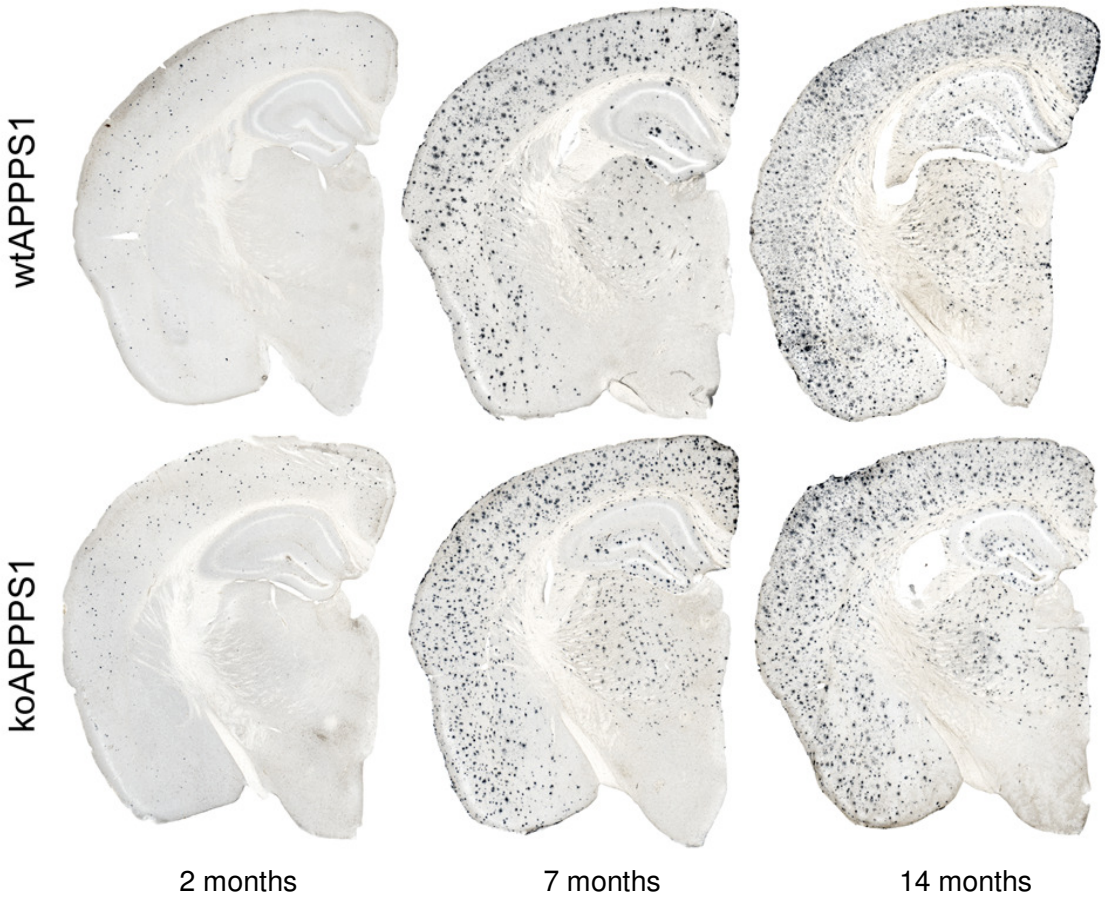


**Fig. 8** Immunohistochemical stainings of human Aβ on sections from 2-, 7-, and 14-months old wtAPPPS1 and koAPPPS1 mice do not show a significant difference in cortical amyloid burden distribution.

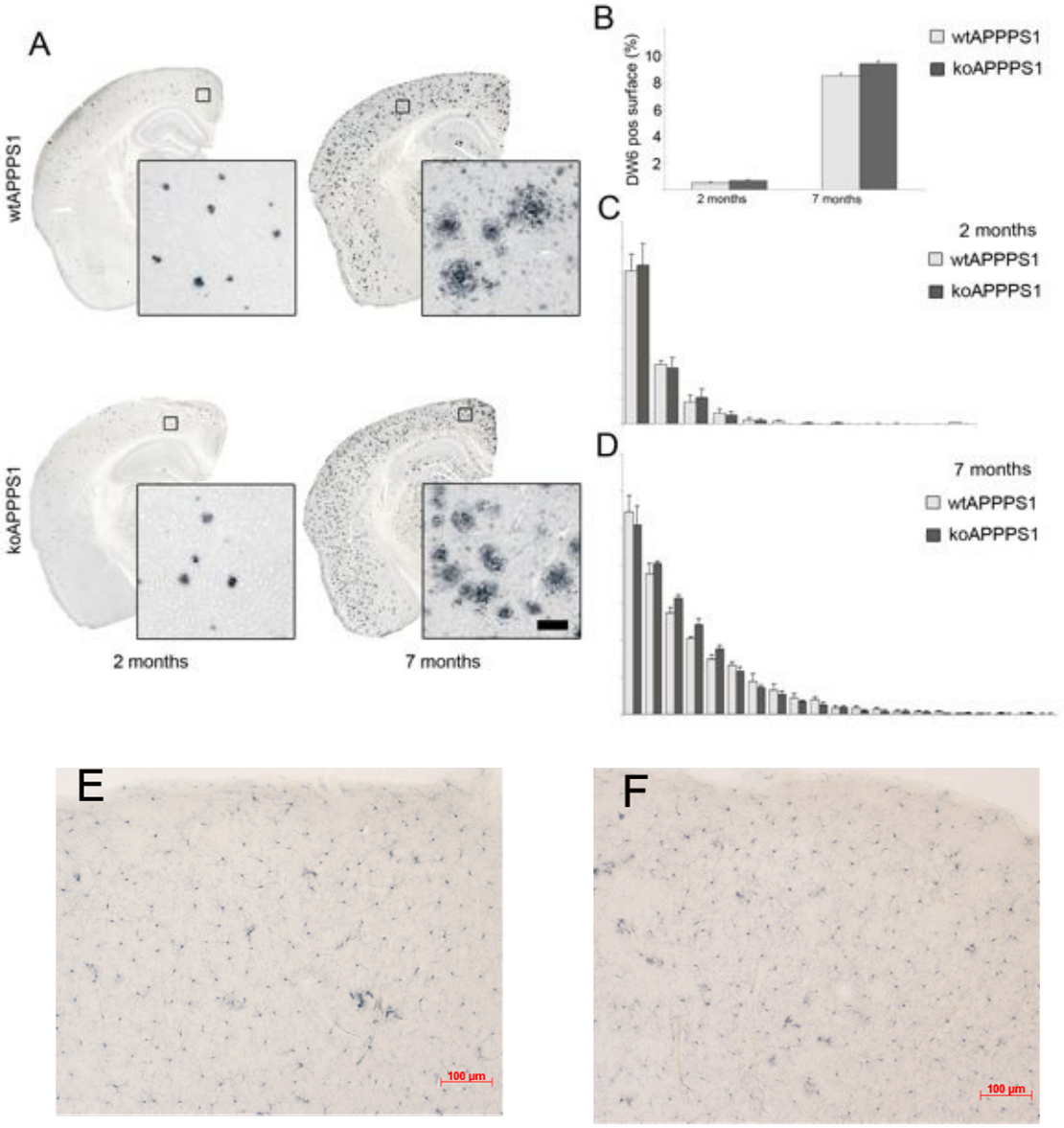


**Fig. 9.** Aβ-immunostainings reveal similar structure of amyloid plaques, degree and pattern of amyloidosis in 2-months old wtAPPPS1 and koAPPPS1 mice. Rectangular boxes indicate the origin of insets. Scale bar represents 50 µm **(A).** 7-mo old wtAPPPS1 mice exhibit amyloid deposits of diffuser type compared to koAPPPS1 mice, although no difference in immunostained area could be assessed on sterological level at 2- and 7-months (2 mo, n = 5 (f1/m4); 7mo, n = 10 (f5/m5)) (p = 0.26). wtAPPPS1- light grey bars and koAPPPS1- dark grey bars **(B).** No difference in plaque size between wtAPPPS1 and koAPPPS1 mice could be found in 2-mo old mice **(C).** 7-mo old wtAPPPS1 mice have larger plaques compared to koAPPPS1 mice (n = 5). Note the enhance of individual plaque size with increasing age **(D).** No significant difference in amyloid-associated gliosis between 2-months old wtAPPPS1 and koAPPPS1 mice

respectively **(E, F).**

### 3.1.3 Increased Aβ levels in koAPPPS1 mice

Brain homogenates from both lines have been analyzed by Western blotting and revealed an increase of total human Aβ levels in koAPPPS1 mice compared to wtAPPPS1 mice at both tested ages (Fig. 10A,B). In 2-mo old koAPPPS1 mice the Aβ levels were doubled, and 7-mo koAPPPS1 mice contain almost one third more Aβ than wtAPPPS1 mice (Fig. 10C).

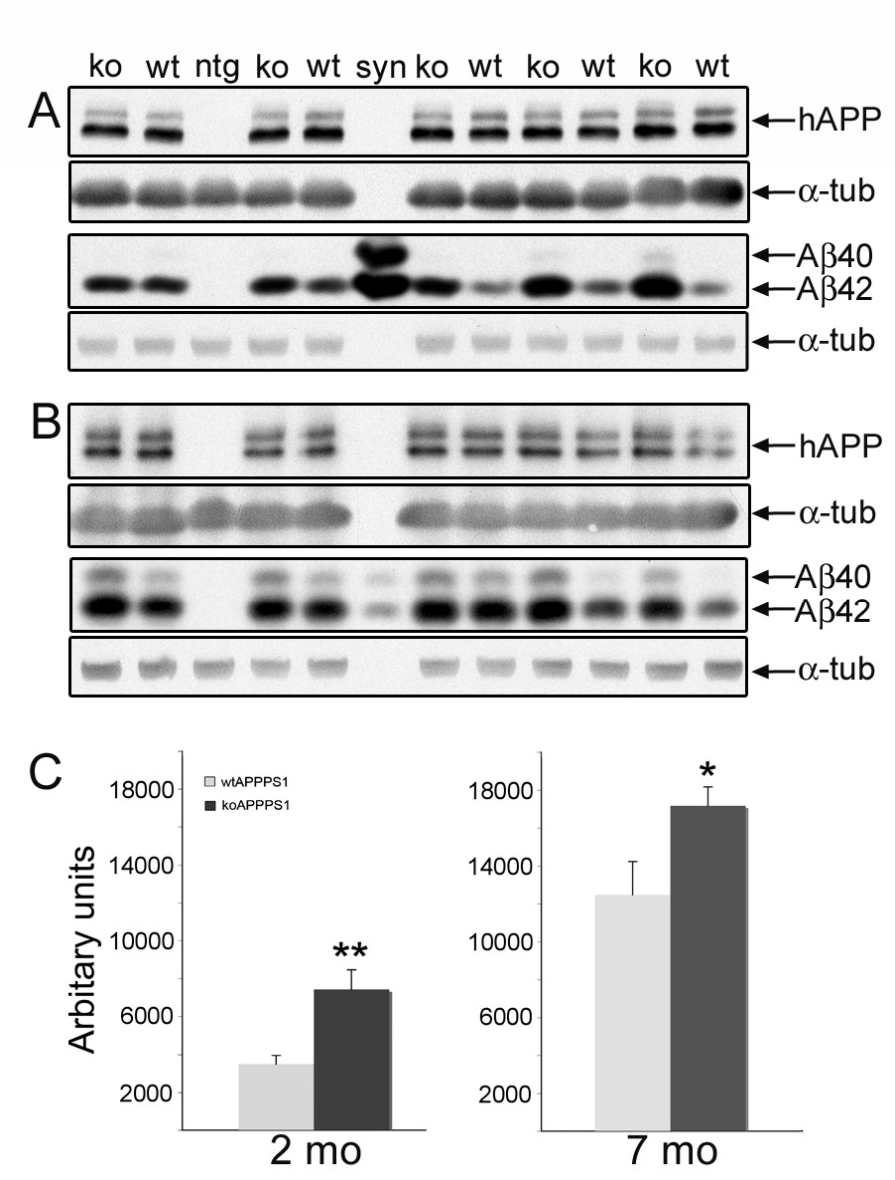


**Fig. 10.** Constant levels of human glycosylated (upper band) and non-glycosylated

(lower band) APP in 2-mo old wtAPPPS1 and koAPPPS1 mice (n = 5; koAPPPS1 and wt APPPS1: m4/f1). The same samples reveal increased Aβ levels in 2-mo old koAPPPS1 mice compared to wtAPPPS1 mice (antibody 6E10). α-tubulin serves as an internal loading control. α-tubulin blots are shown each beyond the corresponding blot **(A).** As in 2-mo old mice expression of human transgenic APP is constant in 7-mo old wtAPPPS1 and koAPPPS1 mice (n = 5; koAPPPS1: f1/m4; wtAPPPS1: f3/m2; p = 0.13), while human Aβ levels were increased in koAPPPS1 compared to wtAPPPS1 mice **(B).** Quantification of Aβ levels from western blots in (A) and (B) indicates significant differences between koAPPPS1 and wtAPPPS1 mice **(C).**

At the same time the transgene derived APP expression levels remained equal in both lines. Elisa analyses confirmed higher Aβ levels in koAPPPS1 mice (Table 3), although the difference between wtAPPPS1 and koAPPPS1 could only be determined as significant in 7-mo old mice. The Aβ42/40 ratios did not change in both lines:

- 2-mo: koAPPPS1 4.8 ± 0.6 vs. wtAPPPS1 5.4 ± 1.6; ± SEM
- 7-mo: koAPPPS1 3.6 ± 0.2 vs. wtAPPPS1 3.3 ± 0.5; ± SEM.

**Table 3.** The amounts of human Aβx-40 and Aβx-42 levels were assessed by enzyme-linked immunosorbent assay in hemibrains lacking cerebellum of 2- to 7-month-old mice. The 2-mo old mice do not show significant different Aβ levels ($p < 0.1$ for Aβ42; $p < 0.1$ for Aβ40). Aβ levels in 7-mo old mice differ significantly in wtAPPPS1 and koAPPPS1 mice ($p < 0.01$ for Aβ42; $p < 0.05$ for Aβ40). No effect of gender on Aβ levels could be observed in 7-mo old mice. (f, female; m, male).

| Age | n | Gender | wtAPPPS1 Aβ40 (pmol/g wet brain) | wtAPPPS1 Aβ42 (pmol/g wet brain) |
|---|---|---|---|---|
| 2 mo | 5 | f1/m4 | 119 ± 25 | 544 ± 75 |
| 7 mo | 10 | f5/m5 | 2104 ± 365 | 6215 ± 949 |

| Age | n | Gender | koAPPPS1 Aβ40 (pmol/g wet brain) | koAPPPS1 Aβ42 (pmol/g wet brain) |
|---|---|---|---|---|
| 2 mo | 5 | f1/m4 | 205 ± 28 | 988 ± 439 |
| 7 mo | 10 | f5/m5 | 3295 ± 336 | 11976 ± 495 |

### 3.1.4 No effect of murine Aß removal on PIB (positron emission tracer Pittburgh Compound B) binding to plaques

For determination of [3H]PiB binding in brain homogenates of wtAPPPS1 and koAPPPS1 mice, ~1 nM [$^3$H]PIB was added to 100 mg/ml of tissue homogenate in the presence and absence of excess cold PiB (1 µM). Nonspecific binding was defined as the number of counts remaining in the presence of 1 µM unlabeled PIB. Brain sample with heavy amyloid from an AD patient has been run in parallel (Table 4). The quantity of [$^3$H]-PIB bound to wtAPPPS1 and to koAPPPS1 brain homogenates does not differ significantly.

**Table 4.** Binding efficiency of the PET tracer PIB to brain samples from an AD patient with heavy amyloid burden and to 15-mo old transgenic mice. Values are mean +/- SD.

| Sample | Total cpm | + 1 µM PiB | Difference | % Specific Binding |
|---|---|---|---|---|
| AD | 8517 ± 191 | 1329 ± 32 | 7188 | 84,4 |
| wtAPPPS | 3893 ± 2.1 | 1383 ± 77 | 2510 | 64.5 |
| koAPPPS | 3610 ± 398 | 1401 ± 42 | 2209 | 61.2 |

## 3.2 A new triple-transgenic mouse model of Alzheimer's disease expressing mutant tau, APP and PS1

The triple transgenic model of Alzheimer's disease with plaques and tangles was generated by crossing the double-transgenic mouse model APPPS1 (APP(swe) and PS1(L166P)) with a single-mutant expressing human P301S tau protein. The resulting progenies have been analyzed.

At 5 months old, no tau immunoreactive nerve cells were present.

13 months old triple transgenic male mice revealed reduced tau pathology compared to the females. Imunohistochemical staining with AT8, that recognizes murine and human tau phosphorylated at Ser202 and Thr205, showed a large number of tau-immunoreactive nerve cells in brainstem and in somatosensory cortex in the triple transgenic mice. In the P301S mice they were also abundant in brainstem (area in which they are usually in the largest number), but in somatosensory cortex the neurofibrillary pathology was less severe (Fig. 11). NFTs were morphologically similar in APPPS1xP301S and P301S mice.

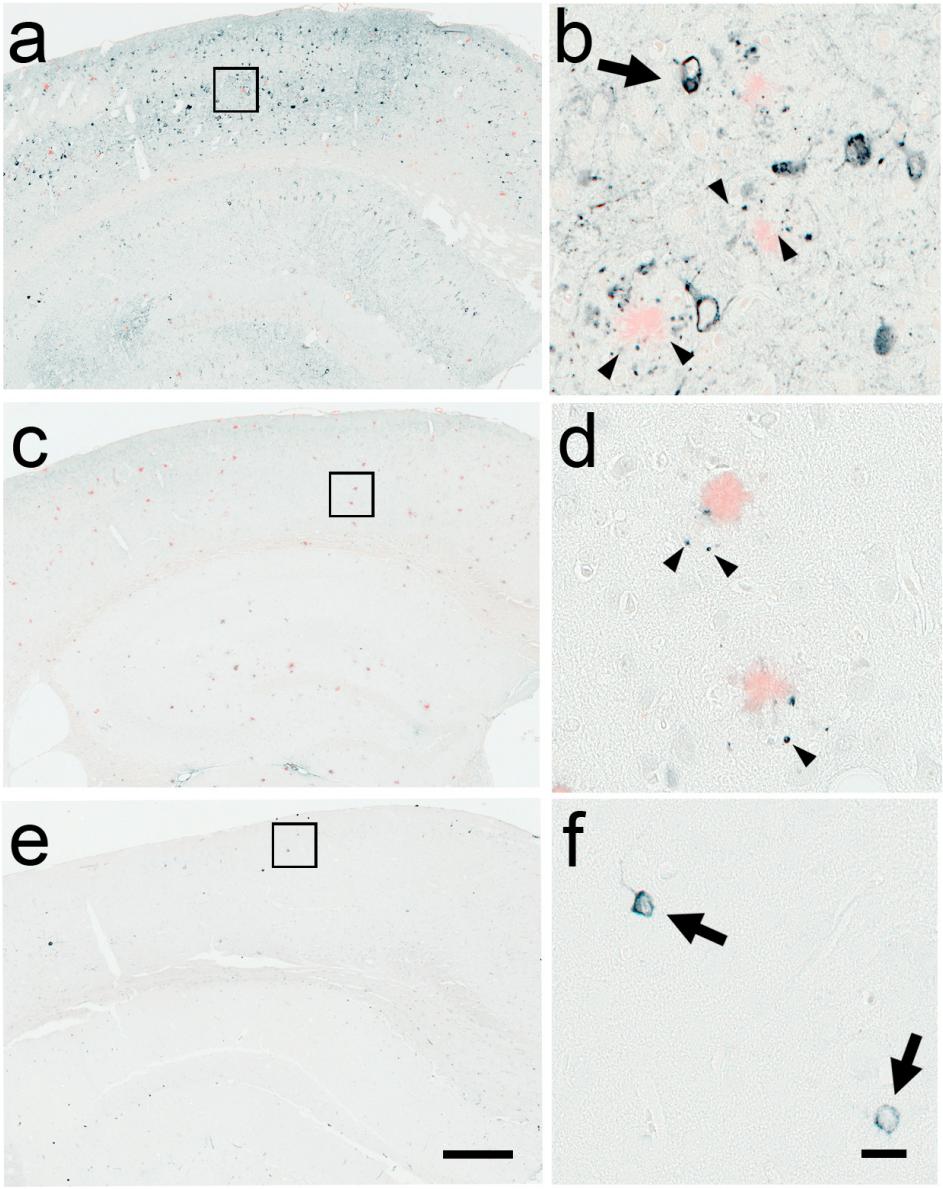


**Fig. 11.** (**a**) Robust tau pathology (black; stained with antibody AT8) and amyloid plaques (red; stained with Congo red) in the somatosensory cortex of triple transgenic mice. (**b**) Higher magnification of the rectangular region delimitated in a shows hyperphosphorylated tau accumulations in dystrophic neurites around amyloid lesion sites (arrowheads). Several neurons reveal fiber like inclusions of hyperphosphorylated tau (arrows). (**c**) In APPPS1 mice, tau lesions are confined to dystrophic neurites around the amyloid deposition sites and consist of mouse tau. Intraneuronal tau accumulations could not be observed in APPPS1 mice. (**d**) Magnification from boxed area in c shows only few immunoreactive neurites (arrowheads) around amyloid deposits compared to double transgenic mice. (**e**) In single transgenic P301S mice

only few neurons are affected by hyperphosphoryted tau inclusions compared to triple transgenics. (**f**) Magnification of marked region in e shows immunoreactive neurons (arrows). Immunostainings were performed on 5 µm paraffin sections. Scale bars are 500 µm (e) and 20 µm (f). Panels a, c, e and panels b, d, f, respectively, have the same magnification. Only sections from female mice are shown (*This figure has been published in the paper: Radde R, Duma C, Goedert M, Jucker M: The value of incomplete mouse models of Alzheimer's disease, Eur J Nucl Med Mol Imaging, 2008 (72)).*

# 4. Discussion

Alzheimer´s disease research proceeds with the use of a variety of transgenic mouse models. They are generated through the overexpression of human mutated APP, with or without additional mutated PS1/2, and/or through the overexpression of mutated tau protein.
With the exception of gene-targeted transgenic models, mouse models are generated against the background of endogenous murine APP. Thus, one purpose of this study was to analyze its influence on cerebral amyloidosis in APPPS1 transgenic mice. Meanwhile, to determine the interaction between Aß and tau, a triple transgenic mouse model, with plaques and tangles has been generated and analyzed.

## 4.1 Murine Aß interferes with the deposition of human Aß

In transgenic AD mouse models, murine Aβ co-integrates in amyloid deposits *(104),* and in vitro, the formation of mixed murine/human amyloid fiber species could be demonstrated *(105).* Thus, the implication of murine Aβ in amyloidosis of transgenic mice is evident, though its impact is poorly understood.
Although the murine Aβ sequence differs from its human counterpart in three amino acid residues *(106),* murine Aβ shares the same amyloidogenic potential of human Aβ in vitro *(107).* In recent studies that discuss the relevance of codepositing murine and human amyloid, it could be shown that the overexpression of wild-type murine APP in APPPS1 transgenic mice led to an increase in cerebral amyloid angiopathy (CAA) and in solubility of the amyloid deposits *(108).* This stands in line with the observation that amyloid deposits isolated from APP transgenic mice are more soluble than human AD plaques *(78, 109).* As a contradict, in vitro formed murine/human mixed amyloid fibers reveal higher insolubility compared to human fibers *(105).* Only amyloid deposits from APP transgenic mice harboring the Aβ affecting Arctic mutation reveal a similar solubility than human AD plaques *(110).*

Plaques from transgenic mice differ from human amyloid deposits also in the following aspects: murine amyloid deposits lack a variety of posttranslational modifications, such as isomerization, racemization, oxidation, and cross-linkage of Aβ peptides *(77)*, and BACE1 cleavage results in preferential cleavage at Aβ amino acid position +11 which results in the deposition of N-terminally truncated Aβ species.

In this study murine Aβ was found in tight association with human fibrillized Aβ in brains of wtAPPPS1 mice, which supports the idea of mixed-species fibril formation *(105).* koAPPPS1 compared to wtAPPPS1 mice showed no change in the site of deposition, age of onset, and neuroinflammatory response, as expected from a previous study *(96).* Further, the Aβ42/40 ratios remain equal in both lines at both sampled ages. Another study examining the contrary scenario with the overexpression of murine APP on an APPPS1 transgenic background resulted in increased CAA levels, a shift in the Aβ ratio towards Aβ40, and higher detergent solubility of aggregates *(108).* No acceleration or exacerbation of cerebral amyloidosis was detected in these mice. Thus, the withdrawal or overproduction of murine Aβ induces more subtle changes such as altered appearance of amyloid deposits as it can be seen in koAPPPS1 mice.

Surprisingly, direct comparison of wtAPPPS1 and koAPPPS1 revealed an increase of total Aβ levels in koAPPPS1 mice. This was unexpected, since wtAPPPS1 mice contain the sum of human and murine APP, and harbor higher APP amounts than koAPPPS1 mice. As its human counterpart, murine APP is processed by β- and γ-secretase to murine Aβ, which co-deposits into transgene induced plaques *(104).*

Higher Aβ levels in koAPPPS1 line can be explained by the amyloid interference hypothesis. According to this, an amyloidogenic peptide which is less prone to aggregate hinders another amyloidogenic peptide from fibrilization. Many studies have proven this assumption. A mouse model that specifically overproduces Aβ40 on an APP transgenic background showed a decreased amyloid burden compared to single transgenic APP mice. The overexpression of the more fibrillogenic Aβ42 promotes amyloidosis, indicating that the potential to form amyloid deposits is also dependent from the proteinous environment .

Similar interference effects were reported from other protein-protein

combinations. The interaction of Cystatin C with Aβ in double transgenic mice leads to decreased amyloid burden compared to single transgenic mice *(111, 112).* Further support for the interference theory comes from double transgenic mice where β-synuclein prevents the more fibrillogenic α-synuclein from aggregation *(113).* Parallel to this discovery, endogenous murine tau was found to delay transgenic human tau aggregation *(114).* All of these studies favour the idea of amyloid interference and emphasize murine Aβ as being preventive against cerebral amyloidosis in transgenic mice.

Although there is strong evidence that the interference of both Aβ species alters the amyloid burden, it cannot be excluded that changes in APP processing lead to increased Aβ levels in koAPPPS1 mice. With the knock-out of endogenous murine APP, only Swedish mutated human APP remains as a substrate for β- and γ-secretase, so human does not compete with murine APP around the two Aβ-forming cleaving enzymes, and as a consequence, the production of human Aβ increases.

Differences between murine and human pathology make it difficult to predict the effects of compounds, therapeutic agents and tracing dyes and impede the interpolation from one onto the other species.

As an example for the need to more insights in human/murine Aβ interference, murine Aβ was falsely suggested to be responsible for inefficient binding capacity to mixed human/murine plaques *(115).* Klunk et al. showed in 2005 that PET radiotracer PIB is retained well in amyloid-containing areas of Alzheimer's disease brain, but not significant in PS1/APP mice even at an age when these mice' brains are loaded with Aβ *(117).* Showing in this study that there is no significant difference in PIB retention between brains of wtAPPPS1 and koAPPPS1 mice, we could prove that not the murine Aβ is causative for this effect and therefore other reasons must be taken into account.

Many promising approaches in order to cure AD work in the mouse model but fail in clinical trials and make the results from in transgenic mice studies questionable. An explanation might consist of these subtle changes that have been identified in this study and should be circumvented by the use of gene-targeted APP knock-out/-in mice.

However, the wtAPPPS1 and koAPPPS1 mice used in this study were not

siblings; therefore these results might have been influenced by a strain difference.
Further research, to investigate the impact of murine APP/Aß on the cerebral amyloidosis of transgenic mice, is required.

## 4.2 Enhanced tau neurofibrillary tangles in triple APP, PS1, and tau transgenic mice

Mouse models that resemble the pathology from the human brain most closely are needed. Such a model has been generated in this study, by breeding APPPS1 transgenic mice with mice expressing P301S mutant tau, and the resulting progeny have been examined.
Triple mutant mice exhibited enhanced neurofibrillary tangle pathology in somatosensory cortex (areas in which, the first amyloid plaques appeared in APPPS1 mice), as compared to single tau mutant mice.
These findings reveal a mechanistic interplay between Aβ and tau, which leads to increased neurofibrillary tangles formation and distribution in regions of brain vulnerable to these lesions, as it has been demonstrated in previous studies too. *(51, 98).*
Notably, plaque formation was not influenced by the presence of the tau lesions. APPPS1 mice developed extracellular Aβ deposits, at the expected age, and prior to tangle formation. This could lead to the conclusion that Aß peptide deposition into senile plaques can cause tau tangles, and tangles do not obligate amyloid plaque formation, according to the amyloid cascade hypothesis. Thus, the interaction of Aß with the P301S mutation was necessary for NFT formation, neither Aß nor the mutation alone being enough to generate high numbers of NFTs *(52).*
Injection of synthetic Aβ42 fibrils or Aβ-rich brain extract into the brains of P301L mutant tau transgenic mice accelerates tangle formation too *(52, 99).* An interaction between Aβ and tau could also be demonstrated through Aβ immunization of triple APP, PS1, and tau transgenic mice, which resulted in a reduction of the tau pathology *(72,117).*

Transgenic mouse models serve as tools in order to study AD and to find a curative treatment against the disease.

# 5. Summary

Alzheimer's disease (AD), a progressive neurodegenerative disorder, is the most common cause of dementia. The neuropathological hallmarks of AD include extracellular deposits of the amyloid-ß peptide (Aß) and neurofibrillary tangles, composed of filamentous aggregates of hyperphosphorylated tau protein.

To study AD pathogenesis, transgenic mice that overexpress human mutated amyloid precursor protein (APP) and/or mutated presenilin1/2 (PS1/2) have been generated. These models exhibit age-related deposition of Aß in the brain parenchyma (amyloid plaques) and in the vasculature (cerebral amyloid angiopathy), and reveal amyloid-associated neuroinflammation, neuritic dystrophy, and synaptic dysfunction. Other characteristics of AD, such as neurofibrillary tangles, are only satisfactorily reproduced in transgenic mouse models that overexpress mutated tau protein.

The first objective of the present work was to study the potential inhibitory effect of murine Aß on human Aß deposition. To this end APP/PS1 double transgenic mice on a wild-type C57BL/6 background have been compared with APP/PS1 mice on an *App*-null background. Comparative ultrastructural and biochemical analysis of these two mouse lines suggested incorporation of mouse Aß in the deposition of human Aß. Surprisingly, an increase of total human Aß levels in APP/PS1 mice on an *App*-null background compared to APP/PS1 mice on a wild-type background has been found. No differences in the site of Aß deposition, age of onset, and amyloid-associated neuroinflammation, and neurodegeneration between the two lines have been observed. Since APP expression and processing was not different between the two lines, the findings suggest that murine Aß interferes with the deposition of human Aß. However, at this point we cannot exclude that the results might be confounded by a selected genetic difference between these two separately maintained lines (albeit in the same environmental conditions).

The second objective was to investigate the interaction between Aß deposits and tau lesions in transgenic mouse models. APP/PS1 double transgenic mice

were crossed with mice expressing P301S mutant tau protein. While Aß deposition in this triple transgenic line was not different from the double APP/PS1 transgenic line, triple transgenic mice exhibited enhanced neurofibrillary tangle pathology compared to single P301S transgenic littermate control mice. These findings suggest a mechanistic interplay between Aß and tau that leads to neurofibrillary tangle formation and provide support for the hypothesis that Aß is the causative factor in AD pathogenesis.

# 6. References

1. Constantine G. Lyketsos, Christopher C. Colenda, Cornelia Beck, Karen Blank, Murali P. Doraiswamy, Douglas A. Kalunian, and Kristine Yaffe, Position statement of the American Association for Geriatric Psychiatry regarding principles of care for patients with dementia resulting from Alzheimer disease. Am J Geriatr Psychiatry (2006) 14:561–72
2. Margaret M. Esiri, James H. Morris, The Neuropathology of Dementia, 1997
3. A. S. Henderson, Epidemiology of Dementia Eur Arch Psychiatry Clin Neurosci (1991) 240 : 205-206
4. Guy McKhann, David Drachman, Marshall Folstein, Robert Katzman, Donald Price and Emanuel M. Stadlan, Clinical diagnosis of Alzheimer's disease: report of the NINCDS-ADRDA Work Group under the auspices of Department of Health and Human Services Task Force on Alzheimer's Disease, Neurology 1984 Jul;34(7):939-44.
5. Evans DA, Funkenstein HH, Albert MS, Scherr PA, Cook NR, Chown MJ, Prevalence of Alzheimer's disease in a community population of older persons. Higher than previously reported, JAMA 1989 Nov 10;262(18):2551-6
6. N. T. Lautenschlager, L. A. Cupples, V. S. Rao, S. A. Auerbach, R. Becker, J. Burke, H. Chui, R. Duara, E. J. Foley, S. L. Glatt, R. C. Green, R. Jones, H. Karlinsky, W. A. Kukull, A. Kurz, E. B. Larson, K. Martelli, A. D. Sadovnick, L. Volicer, S. C. Waring, J. H. Growdon, and L. A. Farrer, Risk of dementia among relatives of Alzheimer's disease patients in the MIRAGE study: What is in store for the oldest old?, Neurology, 1996 Mar;46(3):641-50
7. Lobo A, Launer LJ, Fratiglioni L., Andersen K., Di Carlo A, Breteler M. M. B., Copeland J. R. M., Dartigues J.-F., JAGGER C., Martinez-Lage J., Soininen H., Hofman A, Prevalence of dementia and major subtypes in Europe: A collaborative study of population-based cohorts. Neurologic Diseases in the Elderly Research Group, Neurology, 2000;54(11 Suppl 5):S4-9
8. The prevalence of dementia, Alzheimer's Disease International Factsheet 3 · April 1999
9. C.P. Ferri et al., Global prevalence of dementia: a Delphi consensus study, The Lancet 2005; 366:2112-2117
10. A. Scott Henderson, Anthony F. Jorm, Dementia, Chapter: Definition, and Epidemiology of Dementia, 2002
11. Florence Richard, Philippe Amouyel (2001). Genetic susceptibility factors for Alzheimer's disease.European Journal of Pharmacology 412 2001 1 – 12
12. Finch, C. E., and Tanzi, R. E. (1997). Genetics of aging. Science 278, 407-411
13. Schellenberg GD. Molecular genetics of familial Alzheimer's disease. Arzneimittelforschung. 1995 Mar;45(3A):418-24.
14. Huntington Potter, Am. J. Hum. Genet. 48:1192-1200, 1991, Review and Hypothesis: Alzheimer Disease and Down Syndrome-Chromosome 21 Nondisjunction May Underlie Both Disorders
15. St George-Hyslop, P. H. et al. The genetic defect causing familial Alzheimer's disease maps on chromosome 21. Science 235, 885-90 (1987)
16. Mullan, M. et al. A pathogenic mutation for probable Alzheimer's disease in the APP gene at the N-terminus of beta-amyloid (1992) Nat Genet 1, 345-7

17. Sherrington R, Rogaev EI, Liang Y, Rogaeva EA, Levesque G, Ikeda M, Chi H, Lin C, Li G, Holman K, et al. (1995) Cloning of a gene bearing missense mutations in early-onset familial Alzheimer's disease. Nature 375:754-760
18. Rogaev EI, Sherrington R, Rogaeva EA, Levesque G, Ikeda M, Liang Y, Chi H, Lin C, Holman K, Tsuda T, et al. (1995) ) Familial Alzheimer's disease in kindreds with missense mutations in a gene on chromosome 1 related to the Alzheimer's disease type 3 gene. Nature 376:775-778
19. Goedert M, Spillantini MG ,Tau mutations in frontotemporal dementia FTDP-17 and their relevance for Alzheimer's disease. Biochim Biophys Acta (2000) Jul 26;1502(1):110-21
20. Siddhartha Mondragón-Rodríguez, Gustavo Basurto-Islas, Ismael Santa-Mari, Raúl Mena, Lester I. Binder, Jesús Avila, Mark A. Smith, George Perry, Francisco García-Sierra, Cleavage and conformational changes of tau protein follow phosphorylation during Alzheimer's disease, 2008, Int J Exp Pathol, Apr;89(2):81-9
21. Lyketsos CG, Colenda CC, Beck C, et al. Position statement of the American Association for Geriatric Psychiatry regarding principles of care for patients with dementia resulting from Alzheimer disease, (2006), Am J Geriatr Psychiatry 14:561–72
22. Almkvist O. Neuropsychological features of early Alzheimer's disease: preclinical and clinical stages, (1996) Acta Neurol Scand Suppl 165:63–71
23. Jessica J. Jalbert, Lori A. Daiello and Kate L. Lapane, Dementia of the Alzheimer Type, 2008, Epidemiol Rev. 2008 Jul 16
24. Mayeux, R., and Sano, M. (1999), Treatment of Alzheimer’s disease. N Engl J Med 341, 1670-1679
25. Forstl H, Kurz A. Clinical features of Alzheimer's disease. Eur Arch Psychiatry Clin Neurosci. (1999) 249(6):288-90
26. Clark CM, Karlawish JH. Alzheimer disease: current concepts and emerging diagnostic and therapeutic strategies. Ann Intern Med, (2003) Mar 4;138(5):400-10
27. Colin L. Masters and Konrad Beyreuther, Alzheimer's centennial legacy: prospects for rational therapeutic intervention targeting the Aß amyloid pathway, Brain 2006 129(11):2823-2839
28. Zilka N, Novak M. The tangled story of Alois Alzheimer. Bratisl Lek Listy 2006; 106 (9-10): 3343-345
29. Dennis J. Selkoe,, Alzheimer Disease: Mechanistic Understanding Predicts Novel Therapies, Ann Intern Med. 2004;140:627-638
30. Dennis J. Selkoe and Peter J. Lansbury, Basic Neurochemistry, Part Six. Inherited and Neurodegenerative Diseases, Ch.46, 1999
31. Itagaki, S., McGeer, P. L., Akiyama, H., Zhu, S. & Selkoe, D. Relationship of microglia and astrocytes to amyloid deposits of Alzheimer disease,1989, J Neuroimmunol 24, 173-82
32. Yamada, M. Risk factors for cerebral amyloid angiopathy in the elderly. (2002) Ann N Y Acad Sci 977, 37-44
33. Yoo-Hun Suh and Frederic Checler, Amyloid Precursor Protein, Presenilins, and -Synuclein: Molecular Pathogenesis and Pharmacological Applications in Alzheimer's Disease, (2002) Pharmacol. Rev. 54, 469-525
34. Masters, C. L. et al. Amyloid plaque core protein in Alzheimer disease and Down syndrome, 1985, Proc Natl Acad Sci U S A 82, 4245-9

35. De Strooper B, Aph-1, Pen-2, and Nicastrin with Presenilin generate an active gamma-Secretase complex. Neuron. 2003 Apr 10;38(1):9-12. Review
36. Jarrett, J. T., Berger, E. P., and Lansbury, P. T., Jr. ,1993, Biochemistry 32, 4693-4697
37. Goedert M., Tau protein and the neurofibrillary pathology of Alzheimer's disease, Trends Neurosci, 1993 Nov;16(11):460-5
38. Mandelkow, E., and Mandelkow, E. M. (1995). Microtubules and microtubule-associated proteins. Curr Opin Cell Biol 7, 72-81
39. Goedert M., Neurofibrillary pathology of Alzheimer's disease and other tauopathies, Prog Brain Res 117, 287-306 , 1998
40. Bart De Strooper and James Woodgett, Alzheimer's disease: Mental plaque removal, Nature 423, 392-393 (22 May 2003)
41. Virginia M.-Y. Lee, Tauists and baptists United--Well Almost!, Science 24 August 2001: Vol. 293. no. 5534, pp. 1446-1447
42. Alzheimer's Disease: A Physician's Guide to Practical Management, Edited by Ralph W. Richter, M.D., and Brigitte Zoeller Richter, Dipl.Pharm. Totowa, N.J., Humana Press, 2003
43. Carlo Ballatore, Virginia M.-Y. Lee, John Q. Trojanowski, Tau-mediated neurodegeneration in Alzheimer's disease and related disorders, Nature Reviews Neuroscience 8, 663-672 (September 2007)
44. Braak H, Braak E. Neuropathological stageing of Alzheimer-related changes. Acta Neuropathol (Berl),1991;82(4):239-59
45. Lyness, S. A., Zarow, C. & Chui, H. C. Neuron loss in key cholinergic and aminergic nuclei in Alzheimer disease: a meta-analysis, 2003, Neurobiol Aging 24, 1-23
46. Hardy J, Allsop D. Amyloid deposition as the central event in the etiology of Alzheimer's disease. Trends Pharmacol Sci. (1991) Oct;12(10):383-8
47. Sorrentino G, Bonavita V, Neurodegeneration and Alzheimer's disease: the lesson from tauopathies, Neurol Sci. 2007 Apr;28(2):63-71
48. Naslund J, Haroutunian V, Mohs R, Davis KL, Davies P, Greengard P, Buxbaum JD. Correlation between elevated levels of amyloid beta-peptide in the brain and cognitive decline. JAMA. 2000 Mar 22- 29;283(12):1571-7
49. Andrea Caricasole, Agata Copani, Alessandra Caruso, Filippo Caraci, Luisa Iacovelli, Maria Angela Sortino, Georg C. Terstappen and Ferdinando Nicoletti, The Wnt pathway, cell-cycle activation and beta-amyloid: novel therapeutic strategies in Alzheimer's disease?, Trends Pharmacol Sci. 2003 May;24(5):233-8. Review
50. Colin L. Masters, Roberto Cappai, Kevin J. Barnham and Victor L. Villemagne, Molecular mechanisms for Alzheimer ’s disease: implications for neuroimaging and therapeutics, Journal of Neurochemistry, 2006, 97, 1700–172
51. Jada Lewis, Dennis W. Dickson, Wen-Lang Lin, Louise Chisholm, Anthony Corral, Graham Jones, Shu-Hui Yen, Naruhiko Sahara, Lisa Skipper, Debra Yager, Chris Eckman, John Hardy, Mike Hutton, Eileen McGowan, Enhanced Neurofibrillary Degeneration in Transgenic Mice Expressing Mutant Tau and APP, Science 24 August 2001: Vol. 293. no. 5534, pp. 1487 – 1491
52. J. Götz, F. Chen, J. van Dorpe, R. M. Nitsch Formation of Neurofibrillary Tangles in P301L Tau Transgenic Mice Induced by A42 Fibrils, Science 24 August 2001: Vol. 293. no. 5534, pp. 1491 – 1495
53. Dick Terwel, David Muyllaert, Ilse Dewachter, Peter Borghgraef, Sophie

Croes, Herman Devijver and Fred Van Leuven, Amyloid activates GSK-3beta to aggravate neuronal tauopathy in bigenic mice, Am J Pathol 2008 Mar;172(3):786-98
54. Phiel, C. J., Wilson, C. A., Lee, V. M.-Y & Klein, P. S. Nature 423, 435-439, 2003
55. Bart De Strooper and James Woodgett, Alzheimer's disease: Mental plaque removal, Nature 423, 392-393, 22 May 2003
56. Jessica J. Jalbert, Lori A. Daiello and Kate L. Lapane, Dementia of the Alzheimer Type, Epidemiologic Reviews, July 16, 2008
57. Irena Melnikova, Therapies for Alzheimer's disease, Nature Reviews Drug Discovery 6, 341-342 (May 2007)
58. Martin R. Farlow, Michael L. Miller, Vojislav Pejovic, Treatment Options in Alzheimer'sDisease: Maximizing Benefit, Managing Expectations, Dement Geriatr Cogn Disord 2008;25:408–422
59. Launer LJ. Nonsteroidal anti-inflammatory drugs and Alzheimer disease: what's next? JAMA, Jun 4, 2003; 289(21):2865-7
60. Weggen S, Eriksen JL, Das P, Sagi SA, Wang R, Pietrzik CU, Findlay KA, Smith TE, Murphy MP, Bulter T, Kang DE, Marquez-Sterling N, Golde TE, Koo EH. A subset of NSAIDs lower amyloidogenic Abeta 42 independently of cyclooxygenase activity. Nature (2001) Nov 8;414(6860):212-6
61. Nourhashemi F, Gillette-Guyonnet S, Andrieu S, Ghisolfi A, Ousset PJ, Grandjean H, Grand A, Pous J, Vellas B, Albarede JL: Alzheimer disease: protective factors. Am J Clin Nutr 2000; 71: 643S–649S
62. Simons M, Keller P, De Strooper B, Beyreuther K, Dotti CG, Simons K, Cholesterol depletion inhibits the generation of beta-amyloid in hippocampal neurons, Proc Natl Acad Sci U S A, (1998) May 26;95(11):6460-4
63. Hans-Wolfgang Klafki, Matthias Staufenbiel,Johannes Kornhuberand Jens, Wiltfang,Therapeutic approaches to Alzheimer's disease, Brain (2006), 129, 2840–2855
64. McLean C. A., Cherny R. A., Fraser F. W., Fuller S. J., Smith M. J., Beyreuther K., Bush A. I. and Masters C. L. (1999) Soluble pool of Aß amyloid as a determinant of severity of neurodegeneration in Alzheimer's disease. Ann. Neurol 46, 860–866
65. DeMattos RB, Bales KR, Cummins DJ, Dodart JC, Paul SM, Holtzman DM. Peripheral anti-A beta antibody alters CNS and plasma A beta clearance and decreases brain A beta burden in a mouse model of Alzheimer's disease, Proc Natl Acad Sci U S A, 2001 Jul 17;98(15):8850-5
66. Wilcock DM, DiCarlo G, Henderson D, Jackson J, Clarke K, Ugen KE, Gordon MN, Morgan D, Intracranially administered anti-Abeta antibodies reduce beta-amyloid deposition by mechanisms both independent of and associated with microglial activation, J Neurosci, 2003 May 1;23(9):3745-51
67. Janus C, Pearson J, McLaurin J, Mathews PM, Jiang Y, Schmidt SD, Chishti MA, Horne P, Heslin D, French J, Mount HT, Nixon RA, Mercken M, Bergeron C, Fraser PE, St George-Hyslop P, Westaway D, A beta peptide immunization reduces behavioural impairment and plaques in a model of Alzheimer's disease, 2000, Nature 408:979-982
68. Morgan D, Diamond DM, Gottschall PE, Ugen KE, Dickey C, Hardy J, Duff K, Jantzen P, DiCarlo G, Wilcock D, Connor K, Hatcher J, Hope C, Gordon M, Arendash GW, A beta peptide vaccination prevents memory loss in an animal

model of Alzheimer's disease, 2000, Nature 408:982-985
69. Orgogozo JM, Gilman S, Dartigues JF, Laurent B, Puel M, Kirby LC, Jouanny P, Dubois B, Eisner L, Flitman S, Michel BF, Boada M, Frank A, Hock C, Subacute meningoencephalitis in a subset of patients with AD after Abeta 42 immunization, Neurology, 2003 Jul 8;61(1):46-54
70. Weiner HL, Selkoe DJ, Inflammation and therapeutic vaccination in CNS diseases, Nature, 2002; 420(6917):879-84
71. Nicoll JA, Wilkinson D, Holmes C, Steart P, Markham H, Weller RO, Neuropathology of human Alzheimer disease after immunization with amyloid-beta peptide: a case report, Nat Med, 2003 Apr;9(4):448-52
72. Radde R, **Duma C,** Goedert M, Jucker M: The value of incomplete mouse models of Alzheimer's disease. Eur J Nucl Med Mol Imaging 2008 Mar; 35 Suppl 1:S70-4
73. Tanzi RE, Bertram L. Twenty years of the Alzheimer ’s disease amyloid hypothesis: a genetic perspective. Cell 2005;120:545–55.
74. De Strooper B. Loss-of-function presenilin mutations in Alzheimer disease. Talking Point on the role of presenilin mutations in Alzheimer disease. EMBO Rep 2007;8:141–6.
75. Selkoe DJ, Wolfe MS. Presenilin: running with scissors in the membrane. Cell 2007;131:215–21.
76. Herzig MC, Van Nostrand WE, Jucker M. Mechanism of cerebral beta-amyloid angiopathy: murine and cellular models. Brain Pathol 2006;16:40–54.
77. Roher AE, Kokjohn TA. Appraisal of AbetaPP transgenic mice as models for Alzheimer ’s disease amyloid cascade. Curr Med Chem 2003;3:85–90.
78. Kalback W, Watson MD, Kokjohn TA, Kuo YM, Weiss N, Luehrs DC, et al. APP transgenic mice Tg2576 accumulate Abeta peptides that are distinct from the chemically modified and insoluble peptides deposited in Alzheimer ’s disease senile plaques. Biochemistry 2002;41:922–8.
79. Sturchler-Pierrat C, Abramowski D, Duke M, Wiederhold KH, Mistl C, Rothacher S, et al. Two amyloid precursor protein transgenic mouse models with Alzheimer disease-like pathology. Proc Natl Acad Sci USA 1997;94:13287–92.
80. McGowan E, Sanders S, Iwatsubo T, Takeuchi A, Saido T, Zehr C, et al. Amyloid phenotype characterization of transgenic mice overexpressing both mutant amyloid precursor protein and mutant presenilin 1 transgenes. Neurobiol Dis 1999;6:231–44.
81. Phinney AL, Deller T, Stalder M, Calhoun ME, Frotscher M, Sommer B, et al. Cerebral amyloid induces aberrant axonal sprouting and ectopic terminal formation in amyloid precursor protein transgenic mice. J Neurosci 1999;19:8552–9.
82. Urbanc B, Cruz L, Le R, Sanders J, Ashe KH, Duff K, et al. Neurotoxic effects of thioflavin S-positive amyloid deposits in transgenic mice and Alzheimer ’s disease. Proc Natl Acad Sci USA 2002;99:13990–5.
83. Tsai J, Grutzendler J, Duff K, Gan WB. Fibrillar amyloid deposition leads to local synaptic abnormalities and breakage of neuronal branches. Nat Neurosci 2004;7:1181–3.
84. West MJ, Coleman PD, Flood DG, Troncoso JC. Differences in the pattern of hippocampal neuronal loss in normal ageing and Alzheimer ’s disease. Lancet 1994;344:769–72.

85. Gomez-Isla T, Price JL, McKeel DW Jr, Morris JC, Growdon JH, Hyman BT. Profound loss of layer II entorhinal cortex neurons occurs in very mild Alzheimer's disease. J Neurosci 1996;16:4491–500.
86. Irizarry MC, Soriano F, McNamara M, Page KJ, Schenk D, Games D, et al. Abeta deposition is associated with neuropil changes, but not with overt neuronal loss in the human amyloid precursor protein V717F (PDAPP) transgenic mouse. J Neurosci 1997;17:7053–9.
87. Takeuchi A, Irizarry MC, Duff K, Saido TC, Hsiao Ashe K, Hasegawa M, et al. Age-related amyloid beta deposition in transgenic mice overexpressing both Alzheimer mutant presenilin 1 and amyloid beta precursor protein Swedish mutant is not associated with global neuronal loss. Am J Pathol 2000;157:331–9.
88. Calhoun ME, Wiederhold KH, Abramowski D, Phinney AL, Probst A, Sturchler-Pierrat C, et al. Neuron loss in APP transgenic mice. Nature 1998;395:755–6.
89. Kurt MA, Davies DC, Kidd M, Duff K, Howlett DR. Hyper- phosphorylated tau and paired helical filament-like structures in the brains of mice carrying mutant amyloid precursor protein and mutant presenilin-1 transgenes. Neurobiol Dis 2003;14:89–97.
90. Radde R, Bolmont T, Kaeser SA, Coomaraswamy J, Lindau D, Stoltze L, et al . Abet a42- driven cerebral amyloidosis in transgenic mice reveals early and robust pathology. EMBO Rep 2006;7:940–6.
91. Götz J, Chen F, Barmettler R, Nitsch RM. Tau filament formation intransgenic mice expr essing P301L t au. J Biol Chem 2001;276:529–34.
92. Lewis J, McGowan E, Rockwood J, Melrose H, Nacharaju P, Van Slegtenhorst M, et al. Neurofibrillary tangles, amyotrophy and progressive motor disturbance in mice expressing mutant (P301L) tau protein. Nat Genet 2000;25:402–5.
93. Allen B, Ingram E, Takao M, Smith MJ, Jakes R, Virdee K, et al. Abundant tau filaments and nonapoptotic neurodegeneration in transgenic mice expressing human P301S tau protein. J Neurosci 2002;22:9340–51.
94. Ishihara T, Zhang B, Higuchi M, Yoshiyama Y, Trojanowski JQ, Lee VM. Age-dependent induction of congophilic neurofibrillary tau inclusions in tau transgenic mice. Am J Pathol 2001;158:555–62.
95. Lamb BT, Bardel KA, Kulnane LS, Anderson JJ, Holtz G, Wagner SL, et al. Amyloid production and deposition in mutant amyloid precursor protein and presenilin-1 yeast artificial chromosome transgenic mice. Nat Neurosci 1999;2:695–7.
96. Calhoun ME, Burgermeister P, Phinney AL, Stalder M, Tolnay M, Wiederhold KH, et al. Neuronal overexpression of mutant amyloid precursor protein results in prominent deposition of cerebrovascular amyloid. Proc Natl Acad Sci USA 1999;96:14088–93.
97. Herzig MC, Winkler DT, Burgermeister P, Pfeifer M, Kohler E, Schmidt SD, et al. Abeta is targeted to the vasculature in a mouse model of hereditary cerebral hemorrhage with amyloidosis. Nat Neurosci 2004;7:954–60.
98. Oddo S, Caccamo A, Shepherd JD, Murphy MP, Golde TE, Kayed R, et al. Triple-transgenic model of Alzheimer 's disease with plaques and tangles: intracellular Abeta and synaptic dysfunction. Neuron 2003;39:409–21.
99. Bolmont T, Clavaguera F, Meyer-Luehmann M, Herzig MC, Radde R,

Staufenbiel M, et al. Induction of tau pathology by intracerebral infusion of Abeta-containing brain extract and in APP×tau transgenic mice. Am J Pathol 2007;171:2012–20.
100. Anna K. Stalder, Florian Ermini, Luca Bondolfi, Werner Krenger, Guido J. Burbach, Thomas Deller, Janaky Coomaraswamy, Matthias Staufenbiel, Regine Landmann, and Mathias Jucker, Invasion of Hematopoietic Cells into the Brain of Amyloid Precursor Protein Transgenic Mice, J Neurosci. 2005 Nov 30;25(48):11125-32
101. Luca Bondolfi, Michael Calhoun, Florian Ermini, H. Georg Kuhn, Karl-Heinz Wiederhold, Lary Walker, Matthias Staufenbiel, and Mathias Jucker, Amyloid-associated neuron loss and gliogenesis in the neocortex of amyloid precursor protein transgenic mice, J Neurosci. January 15, 2002, 22(2):515-522
102. Schwarz H and Humbel BM, Correlative light and electron microscopy using immunolabeled resin sections, Methods Mol Bio 2007;369:229-56
103. M. Stalder, T. Deller, M. Staufenbiel, M. Jucker, 3D-Reconstruction of microglia and amyloid in APP23 transgenic mice: no evidence of intracellular amyloid, Neurobiol Aging 2001 May-Jun;22(3):427-34
104. Pype S, Moechars D, Dillen L, & Mercken M, Characterization of amyloid beta peptides from brain extracts of transgenic mice overexpressing the London mutant of human amyloid precursor protein, J Neurochem, 2003; 84(3):602-609
105. Fung J, Frost D, Chakrabartty A, & McLaurin J, Interaction of human and mouse Abeta peptides, J Neurochem 2004, 91(6):1398-1403
106. Yamada T, et al., Complementary DNA for the mouse homolog of the human amyloid beta protein precursor, Biochem Biophys Res Commun, 1987; 149(2):665-671
107. Hilbich C, Kisters-Woike B, Reed J, Masters CL, & Beyreuther K, Human and rodent sequence analogs of Alzheimer's amyloid beta A4 share similar properties and can be solubilized in buffers of pH 7.4, Eur J Biochem, 1991; 201(1):61-69
108. Jankowsky JL, et al., Rodent A beta modulates the solubility and distribution of amyloid deposits in transgenic mice, J Biol Chem, 2007, 282(31):22707-22720
109. Kuo YM, et al., Comparative analysis of amyloid-beta chemical structure and amyloid plaque morphology of transgenic mouse and Alzheimer's disease brains, J Biol Chem, 2001, 276(16):12991-12998
110. Philipson O, et al., A highly insoluble state of Abeta similar to that of Alzheimer's disease brain is found in Arctic APP transgenic mice, Neurobiol Aging 2008.
111. Stephan A Kaeser, Martin C Herzig, Janaky Coomaraswamy, Ellen Kilger, Maj-Linda Selenica, David T Winkler, Matthias Staufenbiel, Efrat Levy, Anders Grubb & Mathias Jucker, Cystatin C modulates cerebral beta-amyloidosis, Nature Genetics 39(12):1437-9. Epub 2007 Nov 18
112. Weiqian Mi, Monika Pawlik, Magdalena Sastre, Sonia S Jung, David S Radvinsky, Andrew M Klein, John Sommer, Stephen D Schmidt, Ralph A Nixon, Paul M Mathews & Efrat Levy, Cystatin C inhibits amyloid-beta deposition in Alzheimer's disease mouse models, Nature Genetics, 2007 Dec;39(12):1440-2. Epub 2007 Nov 18.
113. Makoto Hashimoto, Edward Rockenstein, Michael Mante, Margaret Mallory and Eliezer Masliah, beta-Synuclein inhibits alpha-synuclein aggregation: a

possible role as an anti-parkinsonian factor. Neuron, 2001 Oct 25;32(2):213-23
114. Cathy Andorfer, Yvonne Kress, Marisol Espinoza, Rohan de Silva, Kerry L. Tucker, Yves-Alain Barde, Karen Duff and Peter Davies, Hyperphosphorylation and aggregation of tau in mice expressing normal human tau isoforms, J Neurochem, 2003 Aug;86(3):582-90
115. William E. Klunk, Brian J. Lopresti, Milos D. Ikonomovic, Iliya M. Lefterov, Radosveta P. Koldamova, Eric E. Abrahamson, Manik L. Debnath, Daniel P. Holt, Guo-feng Huang, Li Shao, Steven T. DeKosky, Julie C. Price, and Chester A. Mathis, Binding of the Positron Emission Tomography Tracer Pittsburgh Compound-B Reflects the Amount of Amyloid- in Alzheimer's Disease Brain But Not in Transgenic Mouse Brain, The Journal of Neuroscience, November 16, 2005, 25(46):10598-10606;
116. Selkoe DJ. Alzheimer's disease: genes, proteins, and therapy. Physiol Rev. (2001) Apr;81(2):741-66
117. Oddo S, Billings L, Kesslak JP, Cribbs DH, LaFerla FM. Abeta immunotherapy leads to clearance of early, but not late, hyperphosphorylated tau aggregates via the proteasome. Neuron 2004; 43:321–32.

# 7. Appendix

Parts of this Dissertation have been already published in the paper: Radde R, **Duma C**, Goedert M, Jucker M: *The value of incomplete mouse models of Alzheimer's disease*. Eur J Nucl Med Mol Imaging 2008 Mar; 35 Suppl 1:S70-4, or are going to be published in: **Duma C**, Radde R, Eisele Y, Klunk WE, Mathews PM, Jucker M.: *Murine Abeta interferes with human Abeta in APPPS1 mice (in preparation).*

## 7.1 Acknowledgments

First I would like to specially thank my supervisor Prof. Dr. Mathias Jucker for giving me the opportunity to carry out my scientific study in his research laboratory, and for his excellent advice and guidance.
This study has been supported by a stipend from the Hertie Foundation, Frankfurt, Germany.
Many thanks to Assistant Professor P.M. Mathews (Nathan S. Kline Institute for Psychiatric Research, New York, USA), to Dr. H. Schwarz (Group leader at Max Planck Institute for Developmental Biology, Tübingen, Germany) and to Prof. W.E. Klunk (Department of Psychiatry at the University of Pittsburgh, USA) for their scientific help.
Sincere thanks to Rebecca Radde, Yvonne Eisele, Jörg Odenthal, Stephan Käser and to Tristan Bolmont for their help, guidance and patience. I am also grateful to my former and present colleagues: Amudha Nagarathinam, Bernadette Graus, Bettina Wegenast-Braun, Christian Krüger, Claudia Schäfer, Daniel Eicke, David Milford, Daniela Rosenkranz, Ellen Kilger, Franziska Berke, Götz Heilbronner, Heidrun Wölfing, Isolde Guhl, Janaky Coomaraswamy, Jeannine Kern, Laila Behrends, Michael Calhoun, Ulrike Obermüller, Petra Füger, Simone Eberle, Stefan Grathwohl and Tobias Rasse for being good companions during the daily lab life.
Additionally, I thank my loving family for their invaluable support.
This work is dedicated to the memory of my father, Teodor Duma.